Resistance of E2F4DN to p38^{MAPK} phosphorylation attenuates DNA damage-induced neuronal death via Cited2

Aina María Llabrés-Mas[1], Alberto Garrido-García[1,2], Vanesa Cano-Daganzo[1,2], José M. Frade[1,*]

[1]Department of Molecular, Cellular and Developmental Neurobiology, Cajal Institute, Avenida Doctor Arce 37, 28002 Madrid, Spain; [2] Tetraneuron, Duque de Calabria 12, 46005 Valencia, Spain

*Corresponding autor: frade@cajal.csic.es

Abstract

E2F4, a transcription factor with a prominent role in cell homeostasis, can be phosphorylated by the stress kinase $p38^{MAPK}$ at the Thr248/Thr250 motif, while the Thr248Ala/Thr250Ala E2F4 mutant (E2F4DN) triggers multifactorial therapeutic effects in a murine model of Alzheimer's disease. We hypothesized that the mechanism of action of this therapy relays on the phosphorylation of the Thr248/Thr250 motif under stress conditions, which prevents the homeostatic function of E2F4, while exogenous E2F4DN expression can restore this function. To provide support to this hypothesis, we have focused on genotoxicity induced by camptothecin (CPT) in N2a neuroblastoma-derived neurons, as a paradigm of cell stress followed by cell death. Here we show that, in these cells, $p38^{MAPK}$ becomes activated 6 h after CPT treatment, followed by E2F4 phosphorylation in the Thr248/Thr250 motif. The effect of this phosphorylation in apoptosis was tested by overexpressing wild-type E2F4 (E2F4WT), its Thr248Glu/Thr250Glu phosphomimetic (E2F4CA) or E2F4DN in CPT-treated N2a neurons, followed by quantification of procaspase-3 cleavage. E2F1, which was used as a positive control, induced a statistically-significant increase of procaspase-3 cleavage 32 h after CPT treatment. This was mimicked by either E2F4WT or E2F4CA, while E2F4DN expression inhibited this effect through a Cited2-dependent mechanism. Pharmacological $p38^{MAPK}$ inhibition prevented cell death by E2F4WT but not by E2F4CA, confirming the requirement of E2F4 phosphorylation for cell death in these cells. We conclude that the phosphorylation of E2F4 facilitates the death of N2a neurons carrying DNA damage, while E2F4DN maintains the homeostatic function of E2F4 under stress conditions.

Key words: E2F4, phosphorylation, homeostasis, camptothecin, stress.

Introduction

The transcription factor E2F4 is a member of the E2F family of transcription factors, which also includes E2F1, a canonical regulator of the G1/S phase transition in proliferative cells with capacity to induce cell death in differentiated neurons (Wu *et al.*, 2009a; Zhang *et al.*, 2020). E2F4 was initially described as a cell cycle regulator crucial for the establishment of quiescence in proliferative cells (Conboy *et al.*, 2007). Nevertheless, this transcription facgtor can regulate more than 7,000 genes (Lee *et al.*, 2011) that play important roles in cell differentiation, maintenance of DNA integrity, RNA processing, apoptosis, ubiquitination, and cell stress response. Therefore, E2F4 is currently acknowledged as a major player in cell and tissue homeostasis and tissue regeneration (Stevaux and Dyson, 2002; Crosby & Almasan, 2004; Hsu & Sage, 2016; Ramón-Landreau *et al.*, 2022).

There is growing evidence that E2F4 has a multifactorial impact in neuronal welfare and brain homeostasis (López-Sánchez *et al.*, 2021; 2022), and that this transcription factor may be involved in the physiopathology of neurodegenerative diseases, such as Alzheimer disease (AD), and brain aging (Hsu & Sage, 2016; Ramón-Landreau *et al.*, 2022). E2F4 regulates most of AD-specific gene networks in humans (Ding *et al.*, 2019), and becomes upregulated in human AD neurons (Li *et al.*, 2019) as well as in neurons derived from human induced pluripotent stem cells obtained from familial AD patients (Caldwell *et al.*, 2020). Furthermore, the expression of E2F4 is enriched in blood from MCI and AD (Bottero & Potashkin, 2019). Finally, E2F4 participates in the protective action of memantine and donepezil against cognitive impairment induced by nine common endocrine-disrupting chemicals (Nguyen, 2022).

The regulation of E2F4 is complex, as it can be post-translationally modified through acetylation and methylation (Ramón-Landreau *et al.*, 2022). In addition, E2F4 is

susceptible to become phosphorylated by several protein kinases (Morillo *et al.*, 2012; Paquin *et al.*, 2013; Hsu *et al.*, 2019), and the phosphorylation of E2F4 by the stress kinase $p38^{MAPK}$ within an evolutionary-conserved threonine motif (Thr248/Thr250 in the human sequence and Thr249/Thr251 in mouse) can induce cell cycle re-entry in neurons (Morillo *et al.*, 2012). This latter effect can be induced by a phosphomimetic form of E2F4 carrying Glu residues in substitution of the conserved threonines (referred to as E2F4CA), and inhibited by a dominant negative form of E2F4 (referred to as E2F4DN) carrying alanines instead of the conserved Thr residues (Morillo *et al.*, 2012).

There is indirect evidence that the Thr conserved motif of E2F4 can be phosphorylated in AD-affected human neurons, based on an E2F4-specific proximity-ligation assay (PLA) (López-Sánchez *et al.*, 2022). Moreover, a phospho-Thr249-specific antibody generated in our laboratory was able to detect the phosphorylated form of E2F4 in the brain of homozygous 5xFAD mice (López-Sánchez *et al.*, 2021), a known murine model of Alzheimer's disease (AD) (Oakley et al., 2006) with aggravated phenotype due to the increase of gene dosage (Richard *et al.*, 2015). E2F4 phosphorylation at this conserved motif is not specific from the nervous system. Thus, the phosphorylation of Thr248 in human E2F4 and of Thr259 in the mouse sequence has been detected, in retinal pigment epithelium-derived cells and in embryonic stem cells, respectively (Hsu *et al.*, 2019).

We have demonstrated that E2F4DN is an effective and safe multifactorial therapeutic agent in 5xFAD mice. Among the multiple effects of E2F4DN in these mice, we observed reduction of amyloid deposits, gliosis, inflammation, neuronal death, oxidative stress and neuronal tetraploidization, and prevention of dendritic and synaptic alterations, being able to maintain synaptic long-term potentiation (Sánchez-Puelles *et al.*, 2021). It also extended the life span in both wild-type (WT) and 5xFAD mice,

prevented body weight loss and promoted fur regeneration in senile mice (López-Sánchez *et al.*, 2021; 2022; Ramón-Landreau *et al.*, 2022).

Our current hypothesis for the mechanism of action of E2F4DN is that the phosphorylation of the Thr248/Thr250 motif by the stress kinase $p38^{MAPK}$ prevents the homeostatic function of endogenously-expressed E2F4, while the presence of exogenous E2F4DN can restore this function. In this study, we have begun to test this hypothesis by focusing on Neuro2a (N2a) neuroblastoma cells (Mathews *et al.*, 1976) cultured under low serum conditions to induce neuronal differentiation (therefore, we refer to them as N2a neurons). N2a neurons were treated with camptothecin (CPT) to induce DNA damage, as a mechanism of cell stress followed by cell death in neurons (Morris and Geller, 1996). This effect is potentiated by E2F1 expression in a cell cycle-independent manner (Hofland *et al.*, 2000; Dong *et al.*, 2003; Zhang *et al.*, 2020), while E2F4 can regulate E2F1 function in this cellular stress paradigm (Huang *et al.*, 2019). We found that, under these conditions, $p38^{MAPK}$ activity becomes activated in N2a neurons, and this activation correlates with the phosphorylation of endogenous E2F4 at Thr249, an effect that is prevented by the $p38^{MAPK}$-specific inhibitor SB203580. The significance of E2F4 phosphorylation in apoptosis was tested by overexpressing wild-type E2F4 (E2F4WT), the phosphomimetic form of E2F4 (E2F4CA) or E2F4DN, followed by quantification of procaspase-3 cleavage as a readout of apoptosis. E2F1, which was used as a positive control, induced a statistically-significant increase of procaspase-3 cleavage 32 h after CPT treatment. This was mimicked by either E2F4WT or E2F4CA, while E2F4DN expression inhibited this effect. Pretreatment with SB203580 was able to prevent cell death in E2F4WT but not in E2F4CA, confirming the requirement for cell death of E2F4 phosphorylation. Finally, we provide evidence that Cbp/P300-interacting transactivator with Glu/Asp-rich carboxy-terminal domain 2 (Cited2) is required for the antiapoptotic

effect of E2F4DN in this cellular paradigm. We conclude that the phosphorylation of E2F4 prevents its survival effect via Cited2 in N2a neurons subjected to CPT-dependent genotoxicity while E2F4DN rescue these cells from apoptosis. This provides support to the hypothesis that neuronal expression of E2F4DN maintains the homeostatic function of E2F4 under stress conditions.

Materials and Methods

Antibodies

Primary and secondary antibodies together with detailed information about their manufacturers and dilutions that were used for the different procedures in which they were used are shown in Tables 1 and 2, respectively. The immunopurified rabbit polyclonal antibody recognizing the phosphoThr249 epitope of mouse E2F4 (p-E2F4) was previously described by López-Sánchez *et al.*, (2021).

Adenoviral vectors

The coding sequence of human E2F1 (NCBI accession number NM_005225), preceded by the HA tag, or of human E2F4 (NCBI accession number NM_001950), followed by the 6xHis taq, were synthesized by GenScript and cloned into the pcDNA3 plasmid (Invitrogen) to generate the pE2F1 and pE2F4WT plasmids. Then, two mutations were introduced into the pE2F4WT plasmid to generate the pE2F4DN (Thr248Ala/Thr250Ala) and pE2F4CA (Thr248Glu/Thr250Glu) plasmids. Finally, serotype 5 adenoviral vectors (Ad5) carrying the human E2F1, E2F4WT, E2F4DN, and E2F4CA coding sequences were generated as previously described by Miravet *et al.*, (2014). To this aim, recombinant plasmids were generated for the coding sequence of human each of these

proteins flanked by Adenovirus-specific inverted terminal repeats (ITRs) as well as all the genes necessary to generate the vector, except for E1, which codes for the E1A and E1B proteins. These latter proteins were constitutively expressed by the Q packaging cell line BI-HEK_293A, which was transfected with the respective recombinant plasmids described above. In addition, an Ad5 vector expressing a mouse *Cited2*-specific shRNA carrying EGFP as a reporter (Ad5-m-CITED2-shRNA; Cat. No: shADV-255523) was purchased to Vector Biolabs.

Cell cultures

Mouse N2a cells (Mathews *et al.*, 1976) were maintained in Dulbecco's modified Eagle medium (DMEM) (Gibco) supplemented with 10 % fetal bovine serum (FBS) (Gibco), and 0.5% penicillin/streptomycin (P/S) (Gibco). A maximum of 15 passages were given to each cell batch to maintain the characteristics of the cells. For neuronal differentiation, N2a cells were plated at 20,000 cells/cm^2 in DMEM supplemented with 1% FBS without antibiotics and cultured for 18-20 h before performing the experiments. For immunocytochemistry, cells were plated at the same conditions as above on coverslips (Menzel Glässer, 10 mm) pretreated with 65% nitric acid for 18-20 h, and then extensively washed with MilliQ water and sterilized with absolute ethanol.

Adenoviral transduction

For transduction, N2a neurons were cultured for 48 h in the presence of 85 infectious units (IU)/cell of each Ad5 vector. For co-transduction experiments, 60 IU/cell were used for each Ad5 vector (120 IU in total). Around 75-95% of cells were efficiently transduced with these infectious titers.

DNA damage induction

To induce severe DNA damage to N2a neurons, 10 µM CPT (Cell Signaling Technology), prepared in dimethyl sulfoxide (DMSO), was added to the cultures during different time points depending on the experimental design. CPT is a known topoisomerase I inhibitor (Hsiang *et al*., 1985) that causes double-strand breaks in the replication forks that are associated with DNA replication as well as in the DNA supercoils that are formed during transcription (Liu and Wang, 1987).

p38^{MAPK} and c-Jun N-terminal kinase (JNK) inhibition

The p38^{MAPK} inhibitor SB203580 (Cell Signaling Technology) was used at 10 µg/µl, and the JNK kinase inhibitor SP600125 (Calbiochem) was used at 25 µg/µl. Both inhibitors were prepared in DMSO, and added 1 h before CPT treatment. Control cultures were treated with an equivalent volume of DMSO. Both compounds are competitive inhibitors that bind to the ATP binding pocket of these kinases to prevent their catalytic activity (Cuadrado and Nebreda, 2010; Bennett *et al.*, 2001). Total DMSO concentration in cultures containing CPT plus kinase inhibitors was always below 0.5 %.

RNA extraction and cDNA synthesis

N2a neurons were washed with phosphate buffered saline (PBS) and total RNA was then extracted with Qiazol (Qiagen) following the instructions of the manufacturer. The concentration of RNA in each sample was then measured using NanoDrop One UV-Vis (ThermoFisher Scientific), and 5 µg of total RNA were used for the synthesis of the cDNA in a 20 µl reaction mix containing 4 µl of 5x reaction buffer (Invitrogen), 40 units of

RNAsin (Promega), 250 ng/µl of random primers (Invitrogen), 10 mM dNTPs (Biotools), 10 mM dithiothreitol (DTT) (Invitrogen), and 200 units of SuperScript IV (Invitrogen), following the instructions of the reverse transcriptase manufacturer.

Quantitative RT-PCR (qRT-PCR)

qRT-PCR was performed with the QuantStudio 3 Real-Time PCR system (Thermo Fisher Scientific) using SYBR Green (Cultek) in 15 µl reaction volume containing 1 µl cDNA and the upstream and downstream oligonucleotides (see Table 3) at 10 µM.

Cell extracts

Cultures were placed on ice, washed with ice-cold PBS, and incubated for 3 min with 200 µl of cold extraction buffer containing 20 mM Tris-HCl (Roche) pH 6.8, 1 mM EDTA (Merck), 1% Triton-X100 (Sigma), 0.5% sodium dodecyl sulfate (Sigma-Aldrich), 10 mM β-mercaptoethanol (Sigma-Aldrich), and 1× cOmplete Mini, and EDTA-free, protease inhibitor cocktail (Roche). 1× Phosphatase Inhibitor Cocktail 2 (Sigma-Aldrich) was added to the cell lysing buffer in experiments where preservation of phosphoproteins was mandatory. Cell extracts were then scraped with a rubber policeman and homogenized using a 22G needle. Protein was then quantified using the Protein Assay Dye Reagent Concentrate system (BioRad).

Subcellular fractionation

Subcellular fractionation was performed using a modification of the protocol described by Kanning *et al.*, (2003). Briefly, cultures were placed on ice, washed with ice-cold PBS,

and lysed with 500 µl of cold lysis buffer containing 10 mM HEPES (Sigma-Aldrich) pH 7.6, 10 mM NaCl (Merck), 1 mM KH_2PO_4 (Merck), 5 mM $NaHCO_3$ (Merck), 5 mM EDTA (Merck), 1× cOmplete Mini, and EDTA-free, protease inhibitor cocktail. 1× Phosphatase Inhibitor Cocktail 2 was added to the cell lysing buffer in experiments where preservation of phosphoproteins was mandatory. Cell lysates were then scraped with a rubber policeman and homogenized by 10 passages through a 22G needle, and an aliquot of the cell lysate was kept as a lysate control. Cell nuclei were spun down at 300 × g for 10 min and the nuclear pellet was kept at 4 ºC. The supernatant containing membranes and cytosol was then microfuged at 16,000 × g for 45 min at 4°C. The supernatant (cytosol fraction) was removed and concentrated with Vivaspin 500 Centrifugal Concentrator filters (cutoff, 3 kDa) (Sartorius) as described by the manufacturer. In addition, lysis buffer containing 1% Triton X-100 was added to the pellet (membrane fraction). Finally, nuclear proteins were extracted for 15 min under frequent vortexing in high-salt buffer containing 5 mM HEPES pH 8.0, 420 mM NaCl, 0.25 mM $MgCl_2$ (Merck), 0.1 mM EDTA, 12.5% glycerol (PanReac), 1× cOmplete Mini, EDTA-free, protease inhibitor cocktail, and 1× Phosphatase Inhibitor Cocktail 2. The extract was then centrifuged at 16,000 × g for 10 min at 4°C and the supernatant (soluble nuclear fraction) was kept on ice.

Dephosphorylation assay

A cell extract volume containing 16 µg of protein was incubated for 2 h at 37 ºC in 200 µl 1× FastAP reaction buffer (ThermoFisher Scientific) containing 100 U FastAP thermosensitive alkaline phosphatase (AP) (ThermoFisher Scientific). Then, the reaction was stopped by adding 50 µl of 250 mM EDTA. Finally, reactions were concentrated

with Vivaspin 500 Centrifugal Concentrator filters (cutoff, 3 kDa), as described by the manufacturer.

Western blotting and image analysis

Cell extracts and subcellular fractions obtained as described above or AP-treated proteins were boiled for 5 min in 1× Laemli buffer. The extracts were fractionated by SDS PAGE on acrylamide gels of the appropriate concentration, and transferred to 0.45 µm Immobilon-FL polyvinylidene difluoride (PVDF) transfer membranes (Millipore). The membranes were incubated for 1 h with Intercept (TBS) Blocking Buffer solution (LI-COR) (IBB), and then incubated overnight at 4 °C with the appropriate antibody in IBB. After washing the membranes three times in TBS containing 0.1% Tween 20 (TBS-T), they were incubated for 1 h at RT with a 1/15,000 dilution of secondary antibodies in IBB containing 0.1% Tween 20. Finally, they were washed again with TBS-T as described above, followed by a final wash with TBS. The protein bands were then visualized using the Odyssey CLx Infrared Imaging System (LI-COR). Band intensities were quantified using LicorLite using the "asign shape" command for background subtraction. The intensity for each E2F4-specific band obtained in subcellular fractions was quantified using ImageJ software. The intensity of bands corresponding to proteins of interest were normalized to the intensity of actin or lamin B1 in the same lane.

Immunocitochemistry

Immunocytochemistry was performed in N2a neurons cultured on glass coverslips fixed for 15 min at RT with 4% paraformaldehyde (PFA; Merck). After three washes with PBS, cells were permeabilized and blocked with PBS containing 0.1% Triton-X100 (PBS-T)

supplemented with 10% fetal bovine serum (FBS) (blocking medium) for 1 h. Coverslips were then incubated for 2 h at RT with blocking medium and the appropriate primary antibody. After three washes in PBS-T, coverslips were incubated for 1 h in blocking medium containing the appropriate secondary antibody and 0.1 μg 4',6-diamidine-2'-phenylindole (DAPI; Sigma-Aldrich). After three washes with PBS-T plus one additional washing step with PBS, coverslips were mounted with InmunoSelect Antifade Mounting Medium (Dianova) on glass slides. Images of the cells were taken by confocal microscopy.

Confocal microscopy and image analysis

Confocal images were acquired with a Leica SP5 inverted confocal microscope. In all analyses, a range of 10-35 images of 1 μm thick were taken per stack at 40× magnification so that the entire thickness of the cells present in the microscope field is included, and then the maximum projection was obtained. Images used for the analysis of γH2AX were taken at 40× magnification with 2× zoom.

Image analysis was performed using ImageJ (Fiji). For the analysis of caspase-3 activation, the number of cells positive for caspase-3 cleaved at Asp175 were counted and referred to DAPI labeling. For the analysis of DNA damage foci through γH2AX immunostaining, cells were classified based on the nuclear labeling pattern as well as the number of foci present in their nuclei. For the analysis of the phosphoE2F4 vs. E2F4 ratio, DAPI was used as a reference for cell identification and the same setting was used for both phosphoE2F4 and E2F4 labeling channels. Briefly, after adjusting the "threshold" to define the cell outline, the "fill holes" and the "watershed" commands were used to improve the selection of the cells. Then, the region of interest (ROI) tool was used to measure the "integrated density" of each cell.

Statistical analysis

Statistical analyses were carried out using GraphPad Prism software (version 9). Quantitative data are represented as the mean ± standard error of the mean (SEM). Statistical tests used in this study and the number of independent samples for each experimental group are specified in the figure legends. Differences were considered to be statistically significant with a p-value < 0.05.

Results

Low serum concentration favors neuronal differentiation of N2a neuroblastoma cells

To study the role of E2F4 phosphorylation in neuronal DNA damage response we focused on N2a neuroblastoma cells due to the capacity of this cell line to differentiate as neurons under low serum conditions (Muñoz *et al*., 2003; Wu *et al*., 2009b; Tremblay *et al*., 2010¸ Namsi *et al*., 2018). N2a cells were therefore cultured in the presence of 1% FBS to induce neuronal differentiation (Namsi *et al*., 2018). Under these conditions, N2a cells increased the number of processes resembling dendrites (Fig. S1a), which were immunopositive for the dendrite marker Microtubule-associated Protein 2 (MAP2) (Fig. S1b). Moreover, these cells (which will be hereafter referred to as N2a neurons) expressed both *Syn1*-specific mRNA (Fig. S1c) and Synapsin1 protein (Fig. S1b). Nevertheless, in contrast to the study by Paonessa *et al.*, (2013), which showed increased *Syn1* expression in differentiated N2a neuroblastoma, we observed that this protein and its coding mRNA was expressed at similar levels in both undifferentiated N2a neuroblastoma cells and N2a neurons (Fig S1b,c). In any case, the capacity to express Synapsin 1 makes these cells an

ideal system to express exogenous proteins under the control of the human synapsin1 (*hSyn1*) promoter (Kügler *et al*., 2001).

Expression of E2F4 and its mutant forms E2F4DN and E2F4CA in N2a neurons

We confirmed that N2a neurons were able to express E2F4WT and its mutant forms E2F4DN and E2F4CA, driven by the *hSyn1* promoter. By using an anti-6xHis specific antibody, we verified by immunocytochemistry that E2F4WT-6xHis, E2F4DN-6xHis and E2F4CA-6xHis are widely expressed in N2a neurons 48 hours after transduction with the Ad5.E2F4WT-6xHis, Ad5.E2F4DN-6xHis, and Ad5.E2F4CA-6xHis vectors, respectively (Fig. 1a). Quantification of the percentage of 6xHis-positive cells indicated that above 95% id N2a neurons expressed the aforementioned constructs (Fig. 1b). Moreover, western blot (WB) analysis with the anti-6xHis antibody confirmed the expression of these proteins, which displayed a multiband pattern (Fig. 1c). This suggests that, in N2a neurons, E2F4 can be phosphorylated in multiple residues, as previously described by Ginsberg *et al*. (1994) and Paquin *et al*. (2013). As in these later studies, we found five different bands for this transcription factor (bands *a* to *e*), with different mobility. As expected, the phosphomimetic nature of E2F4CA led to the presence of lower mobility bands, which were also named from *a* to *e*, being bands *b* and c those with the highest intensity (Fig. 1c).

The incubation of the cell extracts with AP demonstrated that most of the bands that were observed in E2F4WT-, E2F4DN-, and E2F4CA-expressing N2a neurons derive from different phosphorylation states of the molecule. In this regard, only two high mobility bands (*d* and *e*) remained in the presence of this enzymatic activity (Fig. 1d), suggesting that one of these two bands contains a post-translational modification different from phosphorylation (Ramón-Landreau *et al*., 2022). Interestingly, the intensity of band

e increased upon AP treatment in extracts from E2F4WT-expressing cells, suggesting that this latter band contains the modified form of E2F4 in unphosphorylated state, which reduces its mobility to become part of band *d* upon phosphorylation. This hypothetical modified form of E2F4 seems to become phosphorylated in the Thr248/Thr250 motif since the incubation of the E2F4DN-derived extracts with AP does not increase the intensity of band *e* in comparison to band *d* (Fig. 1d), while the incubation of the E2F4CA-derived extracts with this enzyme leads to an enrichment of band *d* (Fig. 1d).

Our analysis also indicated that E2F1 expression in N2a neurons results in a multiband pattern (Fig. S2), which is consistent with the phosphorylation of this protein in several residues (Fagan *et al*., 1994; Ivanova *et al*., 2009).

Dynamic localization of E2F4, E2F4DN and E2F4CA in subcellular domains

To analyze the cell compartments where exogenous E2F4WT, E2F4DN, and E2F4CA locate in N2a neurons, we obtained subcellular fractions including membrane, cytosol and nucleus. This analysis indicated that, as expected from a soluble protein, all forms of E2F4 were present in the cytosolic and nuclear compartments (Fig. 2a) while E2F4 was absent from the membrane fraction (not shown). The purity of the cytosolic fraction was confirmed by the specific presence of Ku70 (Fig. S3), a cytoplasmic protein that can translocate to the nucleus (Koike, 2002). In addition, only the nuclear fraction contained Histone H4 (Fig. S3), thus confirming the purity of this latter subcellular fraction. The pattern of band intensities differed between the nuclear fraction and the cytosolic fraction. Bands *c* and *d* were the main phosphorylated states observed in the cytosol for both E2F4WT and E2F4DN, while E2F4CA, in accordance with its phosphomimetic nature, displayed higher levels of phosphorylation in this subcellular compartment as its main bands were *b* and *c* (Fig. 2b). In contrast, a shift towards bands with increased

phosphorylated levels was detected in the nucleus, with different degrees depending on the specific form of E2F4 that was analyzed. Nuclear E2F4CA was mainly in the form of band *b*, while the predominant state of E2F4WT was band *c*. Finally, bands *b*, *c*, and *d* were equally displayed for nuclear E2F4DN, indicative of its reduced capacity to become phosphorylated due to the Thr248Ala/Thr250Ala mutation. The differences of phosphorylation state of E2F4DN and E2F4CA (i.e. higher phosphorylation in E2F4CA vs lower phosphorylation in E2F4DN) suggest that the function of E2F4 as a transcription factor, but also as a homeostatic protein (Ramón-Landreau *et al*., 2022), may differ depending on the phosphorylation state of this latter Thr motif.

To study whether DNA damage may induce specific E2F4 phosphorylation at the Thr248/Thr250 motif, we focused on N2a neurons treated with 10 µM CPT as a paradigm of DNA damage (Hsiang *et al*., 1985). The presence in the culture medium of this topoisomerase I inhibitor for 8 h did not substantially modified the phosphorylation profile observed in N2a neurons (Fig. 2a,b), with the exception of band *d* from E2F4WT, which significantly increased its intensity in the presence of CPT (Fig. 2b). The intensity of this band was not significantly altered in both E2F4DN- and E2F4CA-expressing N2a neurons, suggesting that it results from the phosphorylation of the Thr248/Thr250 motif of E2F4 in response to CPT treatment.

CPT treatment induces p38^{MAPK} activity in N2a neurons

In chick neurons, the stress kinase p38^{MAPK} can phosphorylate E2F4 in the Thr265/Thr267 conserved domain (Morillo *et al*., 2012), which is orthologous of Thr248/Thr250 in human E2F4 and Thr249/Thr251 in mouse E2F4 (notice that we will refer to Thr248/Thr250 in those experiments where the different variants of human E2F4 are expressed using Ad5 vectors, whereas the term Thr249/Thr251 will be used for those

experiments where the phosphorylation state of endogenous mouse E2F4 is evaluated). In a mouse model of AD, E2F4 has been shown to become phosphorylated in Thr249 (López-Sánchez *et al*., 2021), likely being this phosphorylation part of the etiophatology of the disease, which includes $p38^{MAPK}$ activation at its early stages (Zhu *et al*., 2000; Sun *et al*., 2003; Savage *et al*., 2002; Colié *et al*., 2017). These observations suggest that stressful conditions triggering $p38^{MAPK}$ activation may lead to $p38^{MAPK}$-dependent phosphorylation of E2F4. To directly test the hypothesis that E2F4 can be phosphorylated by $p38^{MAPK}$ in the Thr249/Thr251 motif, N2a neurons were treated with 10 µM CPT to induce DNA damage, as a mechanism of cell stress followed by cell death in neurons (Morris and Geller, 1996). We found that, under these conditions, $p38^{MAPK}$ activity becomes gradually activated, an effect that is already evident at 6 h while showing statistically significant differences 8 h after CPT treatment (Fig. 3a,b). This effect, which was based on the dual phosphorylation of $p38^{MAPK}$ on Thr180 and Tyr182 (Raingeaud *et al*., 1995), was specific for $p38^{MAPK}$ since the levels of active c-Jun N-terminal kinases (JNK) were not significantly upregulated at the studied time points (Fig. 3c,d).

$p38^{MAPK}$ specifically phosphorylates Thr249 in endogenous E2F4

To verify that the activation of $p38^{MAPK}$ in N2a neurons treated with 10 µM CPT results in the phosphorylation of endogenous E2F4 in its Thr249/Thr251 motif, we used an antibody that recognizes the phosphoThr249 epitope of mouse E2F4, previously generated in our laboratory (López-Sanchez *et al*., 2021). To this aim, N2a neurons were cultured in the presence of 10 µM CPT for 0 h (untreated control cells), 4 h, 6 h and 8 h. Under these conditions, E2F4 expression levels were increased (Fig. S4). These cultures were then fixed and immunostained with the phospho-specific anti-E2F4 antibody together with an antibody recognizing E2F4 independently of its phosphorylation state,

and then the phosphoE2F4/E2F4 ratio was calculated for each experimental condition. We found that the phospho-E2F4/E2F4 ratio was significantly higher in N2a neurons treated with CPT for 8 h (Fig. 4a,b), in accordance with the significant activation of $p38^{MAPK}$ at this time point (see above). This result is consistent with the significant increase of the band *d*, observed specifically in the cytosol of E2F4WT-, but not E2F4DN- or E2F4CA-expressing N2a neurons treated for 8 h with CTP (Fig. 2a,b).

To directly test whether the Thr249-specific phosphorylation of E2F4 in response to CPT was due to $p38^{MAPK}$, N2a neurons were cultured in the same conditions as above either in the presence of 10 µg/µl SB203580, a $p38^{MAPK}$-specific inhibitor (Cuenda *et al.*, 1995; Gould *et al.*, 1995), or in the presence of 25 µg/µl SP600125, a JNK-specific inhibitor (Bennett *et al.*, 2001), the latter as a control. This analysis indicated that the presence of SB203580, but not SP600125, was able to significantly reduce the phosphorylation of E2F4 at both 6 h and 8 h (Fig. 4a,b), the time points at which $p38^{MAPK}$ activation in response to the CTP treatment was already evident (Fig. 3a,b).

E2F4DN expression prevents CPT-induced cell death in N2a neurons

CPT treatment is known to induce apoptosis (Morris and Geller, 1996), which is potentiated by E2F1 expression in a cell cycle-independent manner (Hofland *et al.*, 2000; Dong *et al.*, 2003; Zhang *et al.*, 2020). Therefore, we performed a time course analysis to evaluate the temporal point at which N2a neurons overexpressing E2F1 start to die in response to CPT, as evidence by caspase-3 activation (Fig. S5). This analysis indicated that a statistically significant increase of apoptosis is first detected in these cells 32 h after CPT treatment (compare Fig. 5 with Fig. S6).

CPT treatment can lead to the degradation of Rb protein and phosphorylation of its family members, p107 and p130 (Fusaro *et al*., 2002; Park *et al*., 2000). Therefore, the release of E2F4 may participate in CPT-induced apoptosis, as all these pocket protein members are known E2F4 interactors (Stevens and La Thangue, 2003). To test whether E2F4 and its phosphorylation at the Thr248/Thr250 motif participates in CPT-induced apoptosis, we cultured N2a neurons transduced with the three forms of E2F4 (E2F4WT, E2F3DN and E2F4CA), followed by CPT treatment for 32 h. In addition, E2F1 expression was used as a positive control in this paradigm. This analysis indicated that, like E2F1, both E2F4WT and E2F4CA were able to induce a statistically significant increase of apoptosis in N2a neurons when co-treated with 10 μM CPT for 32 h (Fig. 5). In contrast, no significant induction of apoptosis was observed in these cells in the presence of E2F4DN (Fig. 5). This suggests that $p38^{MAPK}$-dependent phosphorylation of E2F4 in its Thr248/Thr250 motif is required for the trigger of apoptosis by CPT. To test this hypothesis, N2a neurons were cultured in the presence of the $p38^{MAPK}$ inhibitor SB203580 and then transduced with the different forms of E2F4 and co-treated with 10 μM CPT for 32 h. The presence of SB203580 was able to prevent the apoptotic effect of E2F4WT (Fig. 5), providing support to the hypothesis that the phosphorylation of E2F4 in the Thr248/Thr250 motif allows the induction of apoptosis. This was confirmed by the absence of effect of SB203580 on the apoptotic capacity of E2F4CA (Fig. 5). Furthermore, as expected, the $p38^{MAPK}$ inhibitor did not alter the lack of effect of E2F4DN on apoptosis (Fig. 5).

The antiapoptotic effect of E2F4DN in N2a neurons is independent of DNA repair

DNA damage is known to trigger apoptosis, mainly through a p53-dependent mechanism (Fridman and Lowe, 2003) although it may also rely on the transfer RNAse SLFN11 in

p53 mutant cells (Boon *et al*., 2024). Therefore, the antiapoptotic effect of E2F4DN in CPT-treated N2a neurons might depend primarily on the potential effect of E2F4 to favor DNA repair since it regulates the expression of DNA repair genes (Ramón-Landreau *et al*., 2022). Alternatively, E2F4 might prevent apoptosis in these cells by directly acting on the proapoptotic machinery downstream of DNA damage. To test whether E2F4DN prevents DNA damage in response to CPT treatment, N2a neurons, previously transduced with EGFP, E2F4DN or E2F4CA, where maintained for 32 h in the presence of vehicle or of 10 μM CPT. Then, cultures were fixed and immunostained with an anti-γH2AX antibody to identify double strand DNA breaks (Mah *et al*., 2010). This analysis demonstrated that neither the expression of E2F4DN nor E2F4CA altered the presence of double-stranded DNA breaks as revealed by the γH2AX-specific labeling (Fig. 6a-d). No statistically significant differences were observed in the proportion of CPT-treated N2a neurons lacking γH2AX-specific immunostaining when E2F4DN or E2F4CA was expressed as compared to control cells (Fig. 6b). This was also the case for the proportion of both γH2AX-specific foci (Fig. 6c) and diffuse γH2AX labeling (Fig. 6d). In contrast, N2a neurons maintained under control conditions showed reduced DNA damage profiles when expressing E2F4DN or E2F4CA. This was evidenced by the significant increase of cell nuclei with absence of γH2AX labeling (Fig. 6b) and a reduction of E2F4DN cell nuclei with punctated γH2AX labeling (Fig. 6c) when compared to control N2a neurons. These result indicate that, under physiological conditions, E2F4 is able to prevent DNA damage in N2a neurons, independently of its phosphorylation state. In contrast, the capacity of E2F4 to maintain the integrity of DNA is lost under dramatic DNA damage conditions (i.e. CPT treatment). Therefore, our results indicate that the antiapoptotic effect of E2F4DN in response to CPT-induced DNA damage likely relies on its interaction with the downstream pathways involved in cell death.

Cited2 acts downstream of E2F4DN to prevent CPT-dependent N2a neuronal death

Cited2 is a transcriptional regulator that can be regulated by the crosstalk of E2F1 and E2F4 in response to CPT treatment (Huang *et al*., 2019). Depending on the cellular context, this protein can act either as an antiapoptotic factor (Liu *et al*., 2015; Wu *et al*., 2011), since it can prevent p53 activation (Mattes *et al*., 2017), or as a proapoptotic agent (Su *et al*., 2016; Yoshida *et al*., 2011). Therefore, we hypothesized that Cited2 participates in the control of CPT-dependent cell death by E2F4DN due to the capacity of the latter to induce Cited2 expression. This hypothesis was tested using E2F4WT-, E2F4DN- and E2F4CA-expressing N2a neurons treated for 4 h with CPT to avoid any interference with active $p38^{MAPK}$ since, at this time point, $p38^{MAPK}$ has not yet been activated. This analysis demonstrated that E2F4DN strongly upregulates *Cited2* gene expression 4 h after CPT treatment when compared to both 0 h and 2 h. This contrasts with the inability of E2F4CA to induce *Cited2* expression at this time point (Fig. 7a), thus indicating that Thr248/Thr250 phosphorylation prevents the capacity of E2F4 to express *Cited2*. Accordingly, E2F4WT was not able to upregulate the expression of *Cited2* either, when $p38^{MAPK}$ has not yet been activated (Fig. 7a). Under control conditions, *Cited2* expressions was slightly upregulated 2 h after CPT treatment, but its levels of expression did not increase at the 4h time point.

To test the participation of Cited2 in the prevention by E2F4DN of CPT-dependent cell death, we used an adenoviral vector carrying a *Cited2*-specific shRNA (Ad5-m-CITED2-shRNA). The capacity of this vector to co-express EGFP, allowed us to verify that ~75 % of N2a neurons were transduced (Fig. S8). As expected, this shRNA was able to downregulate the expression of endogenous *cited2* mRNA in N2a neurons (Fig. S7). The transduction of N2a neurons with the Ad5-m-CITED2-shRNA vector confirmed that

Cited2 is required for the prevention of CPT-dependent cell death by E2F4DN in these cells. As a first evidence, the presence of the *Cited2*-specific shRNA was able to potentiate the apoptotic effect of CPT (Fig. 7c). Moreover, we verified that Cited2 participates in the antiapoptotic signaling pathway regulated by E2F4DN, as the presence of *Cited2*-shRNA in CPT-treated N2a neurons prevented the prosurvival effect of E2F4DN (Fig. 7d).

Discussion

In this study we have demonstrated that the transcription factor E2F4 can be detected in different phosphorylation states in N2a neurons, showing a spatial pattern that changes when the nucleus is compared to the cytosol. The phosphorylation pattern of exogenous E2F4 changes in response to CPT treatment, due to the activation of $p38^{MAPK}$, a stress kinase that phosphorylates E2F4 in the cytosol within its Thr248/Thr250 motif. This phosphorylation reduces the capacity of E2F4 to induce *Cited2* expression, thus favoring CPT-dependent apoptosis. The phosphorylation in Thr248/250 facilitates E2F4 to mimic the capacity of E2F1 to act synergistically with CPT to induce apoptosis in N2a neurons. In contrast, E2F4DN cannot be phosphorylated by $p38^{MAPK}$, thus favoring the survival of N2a neurons even under strong CPT-triggered genotoxic stress (Fig. 8).

We have shown that, in N2a neurons, E2F4 can be detected in different phosphorylation states, thus confirming previous results from Paquin *et al*. (2013) in colorectal adenomas and intestinal epithelial cells and from Ginsberg *et al*. (1994) in C33A and U937 cells. Nevertheless, the incubation of the cell extracts with AP resulted in a shift towards two high mobility bands, suggesting that two main forms of E2F4 are present in N2a neurons, likely differing from each other by a covalent modification. This contrasts with the results from Ginsberg *et al*. (1994), who found only one band in C33A

cells treated with λ phosphatase. In N2a neurons, E2F4 could be covalently modified by acetylation of its K96 residue (Ramón-Landreau *et al*., 2022), a modification that would theoretically result in a higher mobility when resolved in SDS-PAGE gels (Georgieva and Sendra, 1999). Alternatively, the cleavage of E2F4 in N2a neurons, resulting in a truncated form, would also show higher mobility. Interestingly, we have provided evidence that the highest mobility band observed in N2a neurons, likely the modified form of E2F4, can become phosphorylated by $p38^{MAPK}$ since the AP treatment increases its intensity.

Our study also revealed a different phosphorylation pattern of E2F4 when nuclear and cytosolic extracts were compared, with enhancement of low-mobility bands in the former subcellular compartment, whose particular identity changed depending on the E2F4 variant. Therefore, the translocation of E2F4 to the nucleus seems to be associated with its phosphorylation state, as demonstrated by Paquin *et al*. (2013) who shown that ERK1/2-mediated phosphorylation of E2F4 on Ser244 and Ser384 promotes its nuclear localization in proliferating intestinal cells.

CPT treatment resulted in the phosphorylation of the modified form of E2F4WT at Thr248, resulting in the increase of the intensity of band *d* in the cytosol. The conclusion that the phosphorylated residue of E2F4 that becomes phosphorylated in response to CPT is Thr248 was supported by the observation that the intensity of band *d* did not change upon CPT treatment in both E2F4DN- and E2F4CA-expressing N2a neurons. In addition, immunostaining of N2a neurons with an antibody specific for the phosphoThr249 epitope of endogenous E2F4 confirmed that CPT induces the phosphorylation of E2F4 at Thr249.

We provide evidence that the phosphorylation of E2F4 in response to CPT is triggered by $p38^{MAPK}$, a finding consistent with previous studies demonstrating that CPT

and Irinotecan, a CPT derivative that also inhibites topoisomerase I, can both induce $p38^{MAPK}$ activity in cancer cells (Lee *et al*., 2002; Pranteda *et al*., 2020), thus indicating that $p38^{MAPK}$ can be specifically activated in response to DNA damage (Raman *et al*., 2007). In this regard, we have confirmed that CPT treatment of N2a neurons results in time-dependent activation of $p38^{MAPK}$ but not of JNK, a related stress kinase. The activation of $p38^{MAPK}$ by CPT was paralleled by detection by immunocytochemistry of the phosphoThr249 epitope in N2a neurons, an effect that could be prevented with the $p38^{MAPK}$-specific inhibitor SB203580 but not by JNK inhibition with SP600125. Interestingly, SB203580 is a known inhibitor of the isoforms p38α and p38β (Sabio *et al*., 2004; Kuma *et al*., 2005), suggesting that these isoforms are those involved in the phosphorylation of E2E4 in response to cellular stress.

$p38^{MAPK}$ activation can act as a switch between prosurvival and proapoptotic signaling depending on the strength of the DNA damage (Phong *et al*., 2010; Gong *et al*., 2010; Rudolf *et al*., 2013). In this regard, highly concentrated CPT treatment represents a strong signal leading to $p38^{MAPK}$-dependent apoptosis (Lee *et al*., 2002; Rudolf *et al*., 2013). The effect of CPT is known to be potentiated by E2F1 in a cell cycle-independent manner (Hofland *et al.*, 2000; Dong *et al.*, 2003; Zhang *et al.*, 2020). In line with these observations, we found that E2F1-overexpressing N2a neurons underwent apoptosis after 32 h treatment with 10 μM CPT. E2F4 has been shown to regulate the proapoptotic effect of E2F1 (Huang *et al*., 2019), but the role of E2F4 phosphorylation in this paradigm was unknown. We have demonstrated in this study that the CPT-dependent apoptotic response can be potentiated by E2F4, depending on its Thr248 phosphorylation state. We have demonstrated that the expression of E2F4CA, the Thr248/Thr250 phosphomimetic form of E2F4, potentiates the CPT-induced apoptosis in N2a neurons, an effect that cannot be prevented by SB203880. In contrast, E2F4WT expression potentiates CPT-dependent

apoptosis in a SB203880- inhibitable form, indicating that the activation of $p38^{MAPK}$ by CPT and subsequent phosphorylation of E2F4 is required for this proapoptotic effect. Another evidence for the phosphorylation by $p38^{MAPK}$ of the Thr248/Thr250 motif of E2F4 as a crucial event necessary for the proapoptotic effect of CPT comes from the observation that the expression of E2F4DN prevents this cell death independently of the presence of SB203580.

Our results have revealed that the mechanism used by E2F4DN to prevent CPT-dependent cell death in N2a neurons does not rely in its capacity to induce the expression of DNA damage repair genes (Ren *et al*., 2002; Ramón-Landreau *et al*., 2022). This lack of repair effect of E2F4DN is likely due to the strong DNA damage triggered by the high concentration of CPT that was used because, in contrast, E2F4DN was indeed able to prevent DNA damage under control conditions. Interestingly, this latter effect of E2F4DN was partially mimicked by E2F4CA, demonstrating that the functional effect of the phosphorylation of E2F4 in the Thr248/Thr250 motif may vary depending on the parameter that is analyzed.

We have shown that the lack of apoptotic effect of E2F4DN in CPT-treated N2a neurons depends on Cited2, a transcriptional regulator that may lead to either apoptosis of cell survival depending on the cell context (Liu *et al*., 2015; Wu *et al*., 2011). This conclusion is based on two different lines of evidence. We have demonstrated that E2F4 upregulates *Cited2* expression in the absence of CPT-dependent $p38^{MAPK}$ activation. Furthermore, *Cited2* knock-down with a specific shRNA potentiated the apoptotic effect of CPT and prevented the antiapoptotic effect of E2F4DN. Interestingly, our results in N2a neurons differ from those by Huang *et al*. (2019), who found an opposed activity of Cited2 in primary cortical neurons (Huang *et al*., 2019). In this latter paradigm, CPT

prevents the capacity of E2F4 to repress the capacity of E2F1 to induce the expression of Cited 2, followed by apoptosis.

In summary, we have uncovered in this study a putative mechanism of action of E2F4DN underlying its multifactorial therapeutic capacity as a homeostasis regulator (Fig. 8). This mechanism, which derives from its resistance to become phosphorylated by $p38^{MAPK}$ under genotoxic stress, may be relevant for AD (López-Sánchez *et al*., 2021; 2022; Ramón-Landreau *et al*., 2022), since the affected neurons in this disease have been shown to undergo genotoxic stress (Nelson and Xu, 2023; Kisby *et al*., 2024).

Acknowledgements

This work has been supported by grants RTI2018-095030-B-I00 and PID2021-128473OB-I00, funded by MCIN/AEI/10.13039/501100011033 and "ERDF A way of making Europe". AML-M has held a FPI contract from Ministerio de Ciencia e Innovación (PRE2019-088907).

Author contribution

Design of the work: JMF. Acquisition of data: AML-M, AG-G and VC-D. Analysis and interpretation of data: AML-M and JMF. Writing of the manuscript: JMF. The authors read and approved the final manuscript.

Data Availability

All data generated or analyzed during this study are included in this published article and its supplementary information files.

Ethics approval

Procedures have been approved by the Bioethics Committee of CSIC.

Conflict of interest

JMF is a shareholder (5.42% equity ownership) of Tetraneuron, a biotech company exploiting his patent on the use of E2F4DN as a therapeutic approach against AD. AG-G and VC-D work for Tetraneuron. AML-M declares no conflict of interest.

References

Bennett BL, Sasaki DT, Murray BW, O'Leary EC, Sakata ST, Xu W, Leisten JC, Motiwala A, Pierce S, Satoh Y, Bhagwat SS, Manning AM, Anderson DW. SP600125, an anthrapyrazolone inhibitor of Jun N-terminal kinase. Proc. Natl. Acad. Sci. USA 98, 13681-13686 (2001).

Boon NJ, Oliveira RA, Körner PR, Kochavi A, Mertens S, Malka Y, Voogd R, van der Horst SEM, Huismans MA, Smabers LP, Draper JM, Wessels LFA, Haahr P, Roodhart JML, Schumacher TNM, Snippert HJ, Agami R, Brummelkamp TR. DNA damage induces p53-independent apoptosis through ribosome stalling. Science 384, 785-792 (2024). doi:10.1126/science.adh7950

Bottero V, Potashkin JA. Meta-analysis of gene expression changes in the blood of patients with mild cognitive impairment and Alzheimer's disease dementia. Int. J. Mol. Sci. 20, 5403 (2019).

Caldwell AB, Liu Q, Schroth GP, Galasko DR, Yuan SH, Wagner SL, Subramaniam S. Dedifferentiation and neuronal repression define familial Alzheimer's disease. Sci. Adv. 6, eaba5933 (2020). doi: 10.1126/sciadv.aba5933

Colié S, Sarroca S, Palenzuela R, Garcia I, Matheu A, Corpas R,. Dotti CG, Esteban JA, Sanfeliu C, Nebreda AR. Neuronal p38α mediates synaptic and cognitive dysfunction in an Alzheimer's mouse model by controlling β-amyloid production. Sci. Rep. 7, 45306 (2017). doi:10.1038/srep45306

Conboy CM, Spyrou C, Thorne NP, Wade EJ, Barbosa-Morais NL, Wilson MD, Bhattacharjee A, Young RA, Tavaré S, Lees JA, Odom DT. Cell cycle genes are the evolutionarily conserved targets of the E2F4 transcription factor. PLoS One 2, e1061 (2007). doi: 10.1371/journal.pone.0001061.

Crosby ME, Almasan, A. Opposing roles of E2Fs in cell proliferation and death. Cancer Biol. Ther. 3, 1208-1211 (2004).

Cuadrado A, Nebreda AR. Mechanisms and functions of p38 MAPK signalling. Biochem. J. 429, 403–417 (2010).

Cuenda A, Rouse J, Doza YN, Meier R, Cohen P, Gallagher TF, Young PR, Lee JC. SB 203580 is a specific inhibitor of a MAP kinase homologue which is stimulated by cellular stresses and interleukin-1. FEBS Lett. 364, 229-233 (1995).

Ding J, Kong W, Mou X, Wang S. Construction of Transcriptional Regulatory Network of Alzheimer’s Disease Based on PANDA Algorithm. Interdiscip. Sci. Comput. Life Sci. 11, 226-236 (2019).

Dong YB, Yang HL, McMasters KM. E2F-1 overexpression sensitizes colorectal cancer cells to camptothecin. Cancer Gene Ther. 10, 168-178 (2003). doi: 10.1038/sj.cgt.7700565

Fagan R, Flint KJ, Jones N. Phosphorylation of E2F-1 modulates its interaction with the retinoblastoma gene product and the adenoviral E4 19 kDa protein. Cell 78, 799-811 (1994). doi: 10.1016/s0092-8674(94)90522-3

Fridman JS, Lowe SW. Control of apoptosis by p53. Oncogene 22, 9030-9040 (2003). doi:10.1038/sj.onc.1207116

Fusaro G, Wang S, Chellappan S. Differential regulation of Rb family proteins and prohibitin during camptothecin-induced apoptosis. Oncogene 21, 4539-4548 (2002). doi: 10.1038/sj.onc.1205551

Georgieva EI, Sendra R. Mobility of acetylated histones in sodium dodecyl sulfate-polyacrylamide gel electrophoresis. Anal. Biochem. 269, 399-402 (1999). doi: 10.1006/abio.1999.4050. PMID: 10222016

Ginsberg D, Vairo G, Chittenden T, Xiao ZX, Xu G, Wydner KL, DeCaprio JA, Lawrence JB, Livingston DM. E2F-4, a new member of the E2F transcription factor family, interacts with p107. Genes Dev. 8, 2665-2679 (1994). doi:10.1101/gad.8.22.2665

Gong X, Liu A, Ming X, Deng P, Jiang Y. UV-induced interaction between p38 MAPK and p53 serves as a molecular switch in determining cell fate. FEBS Lett. 584, 4711-4716 (2010). doi:10.1016/j.febslet.2010.10.057

Gould GW, Cuenda A, Thomson FJ, Cohen P. The activation of distinct mitogen-activated protein kinase cascades is required for the stimulation of 2-deoxyglucose uptake by interleukin-1 and insulin-like growth factor-1 in KB cells. Biochem. J. 311, 735-738 (1995).

Hofland K, Petersen BO, Falck J, Helin K, Jensen PB, Sehested M. Differential cytotoxic pathways of topoisomerase I and II anticancer agents after overexpression of the E2F-1/DP-1 transcription factor complex. Clin. Cancer Res. 6, 1488-1497 (2000).

Hsiang YH, Hertzberg R, Hecht S, Liu LF. Camptothecin induces protein-linked DNA breaks via mammalian DNA topoisomerase I. J. Biol. Chem. 260, 14873-14878 (1985).

Hsu J, Sage J. Novel functions for the transcription factor E2F4 in development and disease. Cell Cycle 15, 3183-3190 (2016).

Hsu J, Arand J, Chaikovsky A, Mooney NA, Demeter J, Brison CM, Oliverio R, Vogel H, Rubin SM, Jackson PK, Sage J. E2F4 regulates transcriptional activation in mouse embryonic stem cells independently of the RB family. Nat. Commun. 10, 2939 (2019). doi: 10.1038/s41467-019-10901-x

Huang T, González YR, Qu D, Huang E, Safarpour F, Wang E, Joselin A, Im DS, Callaghan SM, Boonying W, Julian L, Dunwoodie SL, Slack RS, Park DS. The pro-death role of Cited2 in stroke is regulated by E2F1/4 transcription factors. J. Biol. Chem. 294,8617-8629 (2019). doi:10.1074/jbc.RA119.007941

Ivanova IA, Nakrieko KA, Dagnino L. Phosphorylation by p38 MAP kinase is required for E2F1 degradation and keratinocyte differentiation. Oncogene 28, 52-62 (2009). doi: 10.1038/onc.2008.354

Kanning KC, Hudson M, Amieux PS, Wiley JC, Bothwell M, Schecterson LC. Proteolytic processing of the p75 neurotrophin receptor and two homologs generates C-terminal fragments with signaling capability. J. Neurosci. 23, 5425-5436 (2003). doi: 10.1523/JNEUROSCI.23-13-05425.2003

Kisby GE, Wilson DM 3rd, Spencer PS. Introducing the Role of Genotoxicity in Neurodegenerative Diseases and Neuropsychiatric Disorders. Int. J. Mol. Sci. 25, 7221 (2024). doi:10.3390/ijms25137221

Koike M. Dimerization, translocation and localization of Ku70 and Ku80 proteins. J. Radiat. Res. 43, 223-236 (2002) doi: 10.1269/jrr.43.223

Kügler S, Meyn L, Holzmüller H, Gerhardt E, Isenmann S, Schulz JB, Bähr M. Neuron-specific expression of therapeutic proteins: evaluation of different cellular promoters in recombinant adenoviral vectors. Mol. Cell. Neurosci. 17, 78-96 (2001).

Kuma Y, Sabio G, Bain J, Shpiro N, Márquez R, Cuenda A. BIRB796 inhibits all p38 MAPK isoforms in vitro and in vivo. J. Biol. Chem. 280, 19472-19479 (2005). doi:10.1074/jbc.M414221200

Lee BK, Bhinge AA, Iyer VR. Wide-ranging functions of E2F4 in transcriptional activation and repression revealed by genome-wide analysis. Nucl. Acids Res. 39, 3558-3573 (2011). doi: 10.1093/nar/gkq1313.

Lee S, Lee HS, Baek M, Lee DY, Bang YJ, Cho HN, Lee YS, Ha JH, Kim HY, Jeoung DI. MAPK signaling is involved in camptothecin-induced cell death. Mol. Cells 14, 348-354 (2002).

Li P, Marshall L, Oh G, Jakubowski JL, Groot D, He Y, Wang T, Petronis A, Labrie V. Epigenetic dysregulation of enhancers in neurons is associated with Alzheimer's disease pathology and cognitive symptoms. Nat. Commun. 10, 2246 (2019).

Liu LF, Wang JC. Supercoiling of the DNA template during transcription. Proc. Natl. Acad. Sci. USA 84, 7024-7027 (1987). doi:10.1073/pnas.84.20.7024

Liu YC, Chang PY, Chao CC. CITED2 silencing sensitizes cancer cells to cisplatin by inhibiting p53 trans-activation and chromatin relaxation on the ERCC1 DNA repair gene. Nucleic Acids Res. 43, 10760-10781 (2015). doi: 10.1093/nar/gkv934

López-Sánchez N, Garrido-García A, Ramón-Landreau M, Cano-Daganzo V, Frade JM. E2F4-based gene therapy mitigates the phenotype of the Alzheimer’s disease mouse model 5xFAD. Neurotherapeutics 18, 2484–2503 (2021).

López-Sánchez N, Ramón-Landreau M, Trujillo C, Garrido-García A, Frade JM. A mutant variant of E2F4 triggers multifactorial therapeutic effects in 5xFAD mice. Mol. Neurobiol. 59, 3016-3039 (2022).

Mah LJ, El-Osta A, Karagiannis TC. γH2AX: a sensitive molecular marker of DNA damage and repair. Leukemia 24, 679-686 (2010). doi: 10.1038/leu.2010.6

Mathews RA, Johnson TC, Hudson JE. Synthesis and turnover of plasma-membrane proteins and glycoproteins in a neuroblastoma cell line. Biochem. J. 154, 57-64 (1976). doi: 10.1042/bj1540057

Mattes K, Berger G, Geugien M, Vellenga E, Schepers H. CITED2 affects leukemic cell survival by interfering with p53 activation. Cell Death Dis. 8, e3132 (2017). doi:10.1038/cddis.2017.548

Miravet S, Ontiveros M, Piedra J, Penalva C, Monfar M, Chillón M. Construction, production, and purification of recombinant adenovirus vectors. Methods Mol. Biol. 1089, 159-173 (2014). doi: 10.1007/978-1-62703-679-5_12

Morillo SM, Abanto EP, Román MJ, Frade JM. Nerve growth factor-induced cell cycle reentry in newborn neurons is triggered by p38MAPK-dependent E2F4 phosphorylation. Mol. Cell. Biol. 32, 2722-2737 (2012).

Morris EJ, Geller HM. Induction of neuronal apoptosis by camptothecin, an inhibitor of DNA topoisomerase-I: evidence for cell cycle-independent toxicity. J. Cell. Biol. 134, 757-770 (1996). doi: 10.1083/jcb.134.3.757

Muñoz JP, Sánchez JR, Maccioni RB. Regulation of p27 in the process of neuroblastoma N2A differentiation. J. Cell Biochem. 89, 539-549 (2003). doi:10.1002/jcb.10525

Namsi A, Nury T, Hamdouni H, Yammine A, Vejux A, Vervandier-Fasseur D, Latruffe N, Masmoudi-Kouki O, Lizard G. Induction of neuronal differentiation of murine N2a cells

by two polyphenols present in the mediterranean diet mimicking neurotrophins activities: resveratrol and apigenin. Diseases 6, 67 (2018). doi: 10.3390/diseases6030067

Nelson TJ, Xu Y. Sting and p53 DNA repair pathways are compromised in Alzheimer's disease. Sci. Rep. 13, 8304 (2023). doi:10.1038/s41598-023-35533-6

Nguyen HD. Combination of donepezil and memantine attenuated cognitive impairment induced by mixed endocrine-disrupting chemicals: an in silico study. Neurotox. Res. 40, 2072-2088 (2022). doi:10.1007/s12640-022-00591-7

Oakley H, Cole SL, Logan S, Maus E, Shao P, Craft J, Guillozet-Bongaarts A, Ohno M, Disterhoft J, Van Eldik L, Berry R, Vassar R. Intraneuronal beta-amyloid aggregates, neurodegeneration, and neuron loss in transgenic mice with five familial Alzheimer's disease mutations: potential factors in amyloid plaque formation. J. Neurosci. 26,10129-10140 (2006). doi:10.1523/JNEUROSCI.1202-06.2006

Paonessa F, Latifi S, Scarongella H, Cesca F, Benfenati F. Specificity protein 1 (Sp1)-dependent activation of the synapsin I gene (SYN1) is modulated by RE1-silencing transcription factor (REST) and 5'-cytosine-phosphoguanine (CpG) methylation. J. Biol. Chem. 288, 3227-3239 (2013). doi: 10.1074/jbc.M112.399782

Paquin MC, Cagnol S, Carrier JC, Leblanc C, Rivard N. ERK-associated changes in E2F4 phosphorylation, localization and transcriptional activity during mitogenic stimulation in human intestinal epithelial crypt cells. BMC Cell Biol. 14, 33 (2013). doi: 10.1186/1471-2121-14-33

Park DS, Morris EJ, Bremner R, Keramaris E, Padmanabhan J, Rosenbaum M, Shelanski ML, Geller HM, Greene LA. Involvement of retinoblastoma family members and E2F/DP complexes in the death of neurons evoked by DNA damage. J. Neurosci. 20, 3104-3114 (2000). doi: 10.1523/JNEUROSCI.20-09-03104.2000

Phong MS, Van Horn RD, Li S, Tucker-Kellogg G, Surana U, Ye XS. p38 mitogen-activated protein kinase promotes cell survival in response to DNA damage but is not required for the G(2) DNA damage checkpoint in human cancer cells. Mol. Cell. Biol. 30, 3816-3826 (2010). doi:10.1128/MCB.00949-09

Pranteda A, Piastra V, Stramucci L, Fratantonio D, Bossi G. The p38 MAPK Signaling Activation in Colorectal Cancer upon Therapeutic Treatments. Int. J. Mol. Sci. 21, 2773 (2020).

Raingeaud J, Gupta S, Rogers JS, Dickens M, Han J, Ulevitch RJ, Davis RJ. Pro-inflammatory cytokines and environmental stress cause p38 mitogen-activated protein kinase activation by dual phosphorylation on tyrosine and threonine. J. Biol. Chem. 270, 7420-7426 (1995). doi: 10.1074/jbc.270.13.7420

Raman M, Earnest S, Zhang K, Zhao Y, Cobb MH. TAO kinases mediate activation of p38 in response to DNA damage. EMBO J. 26, 2005-2014. (2007). doi:10.1038/sj.emboj.7601668

Ramón-Landreau M, Sánchez-Puelles C, López-Sánchez N, Lozano-Ureña A, Llabrés-Mas AM, Frade JM. E2F4DN transgenic mice: a tool for the evaluation of E2F4 as a therapeutic target in neuropathology and brain aging. Int. J. Mol. Sci. 23, 12093 (2022).

Ren B, Cam H, Takahashi Y, Volkert T, Terragni J, Young RA, Dynlacht BD. E2F integrates cell cycle progression with DNA repair, replication, and G_2/M checkpoints. Genes Dev. 16, 245-256 (2002). doi:10.1101/gad.949802

Richard BC, Kurdakova A, Baches S, Bayer TA, Weggen S, Wirths O. Gene dosage dependent aggravation of the neurological phenotype in the 5xFAD mouse model of Alzheimer's disease. J. Alzheimers Dis. 45, 1223-1236 (2015). doi: 10.3233/JAD-143120. PMID: 25697701

Rudolf E, Kralova V, Rudolf K, John S. The role of p38 in irinotecan-induced DNA damage and apoptosis of colon cancer cells. Mutat. Res. 741-742, 27-34 (2013). doi:10.1016/j.mrfmmm.2013.02.002

Sabio G, Reuver S, Feijoo C, Hasegawa M, Thomas GM, Centeno F, Kuhlendahl S, Leal-Ortiz S, Goedert M, Garner C, Cuenda A. Stress- and mitogen-induced phosphorylation of the synapse-associated protein SAP90/PSD-95 by activation of SAPK3/p38gamma and ERK1/ERK2. Biochem. J. 380, 19-30 (2004). doi:10.1042/BJ20031628

Sánchez-Puelles C, Perea G, Frade JM. E2F4DN-based gene therapy recovers long-term potentiation and hippocampal-dependent memory in homozygous 5xFAD mice. Alzheimers Dement. 17(Suppl.9), e057668 (2021).

Savage MJ, Lin YG, Ciallella JR, Flood DG, Scott RW. Activation of c-Jun N-terminal kinase and p38 in an Alzheimer's disease model is associated with amyloid deposition. J. Neurosci. 22, 3376-3385 (2002). doi:10.1523/JNEUROSCI.22-09-03376.2002

Stevaux O, Dyson NJ. A revised picture of the E2F transcriptional network and RB function. Curr. Op. Cell Biol. 14, 684-691 (2002).

Stevens C, La Thangue NB. E2F and cell cycle control: a double-edged sword. Arch. Biochem. Biophys. 412, 157-169 (2003). doi: 10.1016/s0003-9861(03)00054-7

Su D, Song JX, Gao Q, Guan L, Li Q, Shi C, Ma X. Cited2 participates in cardiomyocyte apoptosis and maternal diabetes-induced congenital heart abnormality. Biochem. Biophys. Res. Commun. 479, 887-892 (2016). doi:10.1016/j.bbrc.2016.09.101

Sun A, Liu M, Nguyen XV, Bing G. P38 MAP kinase is activated at early stages in Alzheimer's disease brain. Exp. Neurol. 183, 394-405 (2003). doi:10.1016/s0014-4886(03)00180-8

Tremblay RG, Sikorska M, Sandhu JK, Lanthier P, Ribecco-Lutkiewicz M, Bani-Yaghoub M. Differentiation of mouse Neuro 2A cells into dopamine neurons. J. Neurosci. Methods. 186, 60-67 (2010). doi:10.1016/j.jneumeth.2009.11.004

Wu PY, Lin YC, Chang CL, Lu HT, Chin CH, Hsu TT, Chu D, Sun SH. Functional decreases in P2X7 receptors are associated with retinoic acid-induced neuronal differentiation of Neuro-2a neuroblastoma cells. Cell Signal. 21, 881-891 (2009a). doi:10.1016/j.cellsig.2009.01.036

Wu ZZ, Sun NK, Chao CC. Knockdown of CITED2 using short-hairpin RNA sensitizes cancer cells to cisplatin through stabilization of p53 and enhancement of p53-dependent apoptosis. J. Cell Physiol. 226, 2415-2428 (2011).

Wu Z, Zheng S, Yu Q. The E2F family and the role of E2F1 in apoptosis. Int. J. Biochem. Cell Biol. 41, 2389-2397 (2009b). doi: 10.1016/j.biocel.2009.06.004

Yoshida T, Sekine T, Aisaki K, Mikami T, Kanno J, Okayasu I. CITED2 is activated in ulcerative colitis and induces p53-dependent apoptosis in response to butyric acid. J. Gastroenterol. 46, 339-349 (2011). doi:10.1007/s00535-010-0355-9

Zhang Y, Song X, Herrup K. Context-dependent functions of E2F1: cell cycle, cell death, and DNA damage repair in cortical neurons. Mol. Neurobiol. 57, 2377-2390 (2020). doi: 10.1007/s12035-020-01887-5

Zhu X, Rottkamp CA, Boux H, Takeda A, Perry G, Smith MA. Activation of p38 kinase links tau phosphorylation, oxidative stress, and cell cycle-related events in Alzheimer disease. J. Neuropathol. Exp. Neurol. 59, 880-888 (2000). doi:10.1093/jnen/59.10.880

Tables

Table 1. Primary antibodies

Protein	Manufacturer	Reference	Host	Application	Dilution
E2F4	Millipore	MABE160	Mouse	ICQ WB	1:200 1:2000
P-E2F4			Rabbit	ICQ	1:50
p-p38	Cell Signaling	4511	Rabbit	WB	1:1000
p38	Cell Signaling	8690	Rabbit	WB	1:2000
Cleaved Caspase-3 (Asp175)	Cell Signaling	9661	Rabbit	ICQ	1:150
6xHis tag	Abcam	ab18184	Mouse	WB	1:1000
Lamin B1	Abcam	ab133741	Rabbit	WB	1:4000
Actin	Millipore	MAB1501R	Mouse	WB	1:10000
E2F1	Santa Cruz	sc-251	Mouse	WB	1:500
p-JNK	Cell Signaling	9252	Rabbit	WB	1:1000
JNK	Cell Signaling	9251S	Rabbit	WB	1:1000
EGFP	Nacalai Tesque	04404-84	Rat	ICQ	1:500
γ H2AX	Abcam	ab26350	Mouse	ICQ	1:300
Map 2	Abcam	ab5392	Chicken	ICQ	1:250
Cited 2	Abcam	ab108345	Rabbit	WB	1:1000
Synapsin 1	Abcam	ab64581	Rabbit	ICQ	1:400
Histone H4	Abcam	ab17036	Mouse	WB	1:2000
Ku70	Santa Cruz Biotechnology	sc-17789	Mouse	WB	1:1000

Table 2. Secondary antibodies

Antibody	Host	Conjugated with	Manufacturer	Reference	Aplication	Dilution
Anti-mouse	Donkey	Alexa 647	Invitrogen (Life Technologies)	A31571	ICQ	1/1000
Anti-mouse	Goat	Alexa 594	Invitrogen (Life Technologies)	A11032	ICQ	1/1000
Anti-mouse	Goat	Alexa 568	Invitrogen (Life Technologies)	A21043	ICQ	1/1000
Anti-mouse	Goat	IRDye 680RD	Li-cor	926-68070	WB	1/7500
Anti-rabbit	Goat	Alexa 568	Invitrogen (Life Technologies)	A11036	ICQ	1/1000
Anti-rabbit	Donkey	Alexa 488	Invitrogen (Life Technologies)	A21206	ICQ	1/1000
Anti-rabbit	Goat	IRDye 800CW	Li-cor	926-32211	WB	1/7500
Anti-rat	Goat	Alexa 647	Invitrogen (Life Technologies)	A21247	ICQ	1/1000

Table 3. Oligonucleotides used in qPCR

Transcript	Species	Position (bp)	NCBI accesión #	Size (bp)	Sequence 5' –> 3'
Rps18	*M. musculus*	120-139	NM_011296	73	**U:** AATAGCCTTCGCCATCACTG
		173-192			**D:** GTCTGCTTTCCTCAACACCA
Cited2	*M. musculus*	878-897	NM_010828	76	**U:** CGCCCAATGTCATAGACACT
		932-953			**D:** CGGTCCAAACCCATTTCTATCA
Syn1	*M. musculus*	2108-2129	NM_013680.4	103	**U:** AGCTCAACAAATCCCAGTCTCT
		2191-2210			**D:** CGGATGGTCTCAGCTTTCAC

Figures

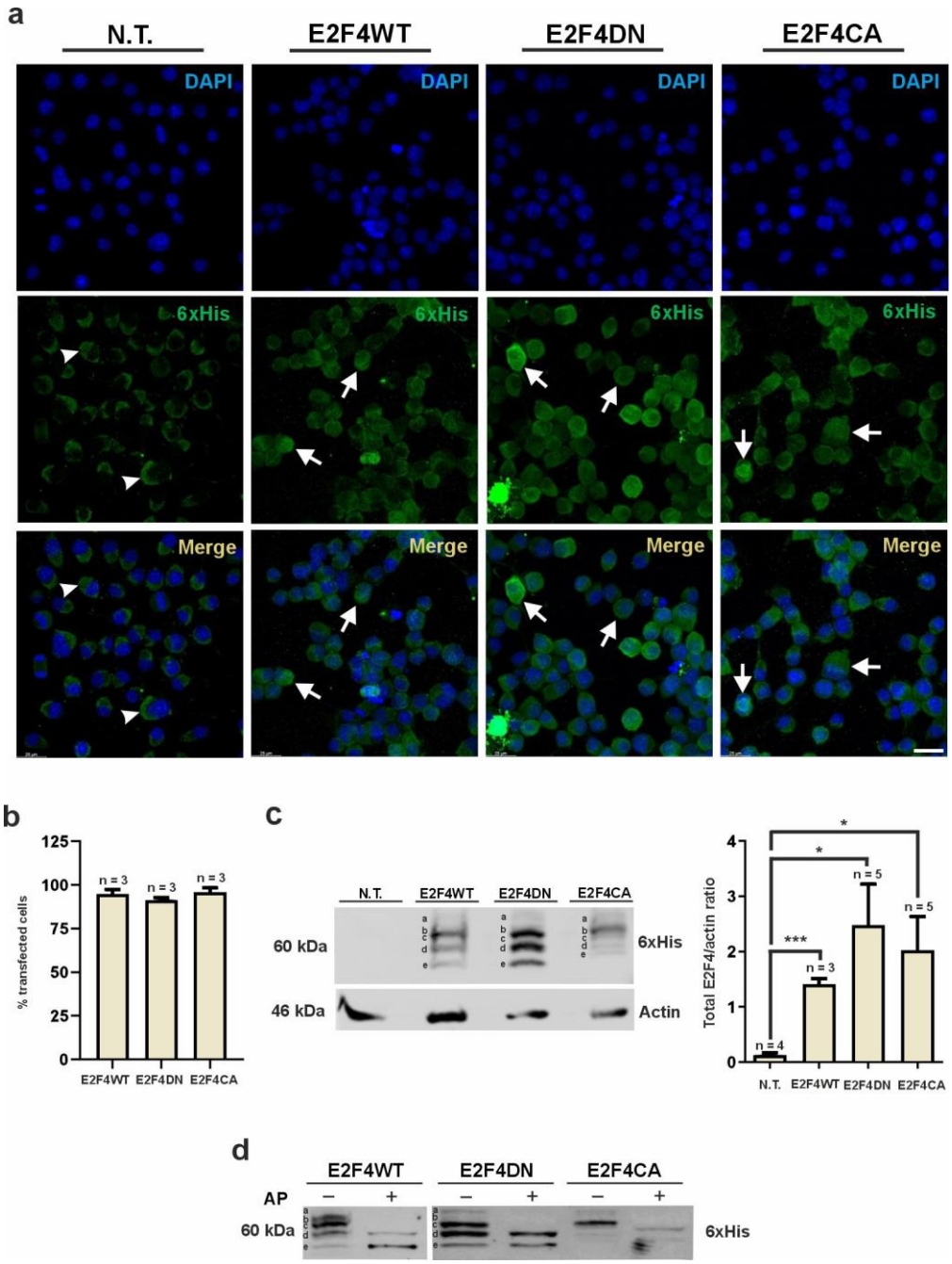

Figure 1. Overexpression and phosphorylation of different E2F4 forms in N2a neurons. (a) Representative inmunostaining of N2a neurons, either non-transfected (N.T.) or transduced with Ad5 vectors expressing E2F4WT-6xHis (E2F4WT), E2F4DN-6xHis (E2F4DN) or E2F4CA-6xHis (E2F4CA), using an anti-6xHis antibody (green). Notice that, while unspecific fluorescence can be observed in the non-transfected cells (arrowhead), 6xHis-specific labeling with different intensity levels was observed in the

transfected cells (arrows). Cell nuclei were labeled with DAPI (blue). Bar: 25 μM. (b) Quantification of E2F4WT-6xHis, E2F4DN-6xHis and E2F4CA-6xHis transduction efficiency in the N2 neuronal cultures shown in a (i.e. number of 6xHis+ cells related to DAPI+ nuclei). (c) Left panel: representative western blot of the multiband pattern (bands a-f) observed in cell extracts from E2F4WT-6xHis, E2F4DN-6xHis or E2F4CA-6xHis-transduced N2a neurons, as revealed with an anti-6xHis antibody. Actin was used as a loading marker. Right panel: quantification of the sum of intensities for the different bands shown in the left panel relativized to actin. *$p<0.05$; ***$p< 0.001$ (unpaired Student's *t* test). (d) Representative western blots of the effect of alkaline phosphatase (AP) on the multiband pattern observed in cell extracts from E2F4WT-6xHis-, E2F4DN-6xHis- or E2F4CA-6xHis-transduced N2a neurons.

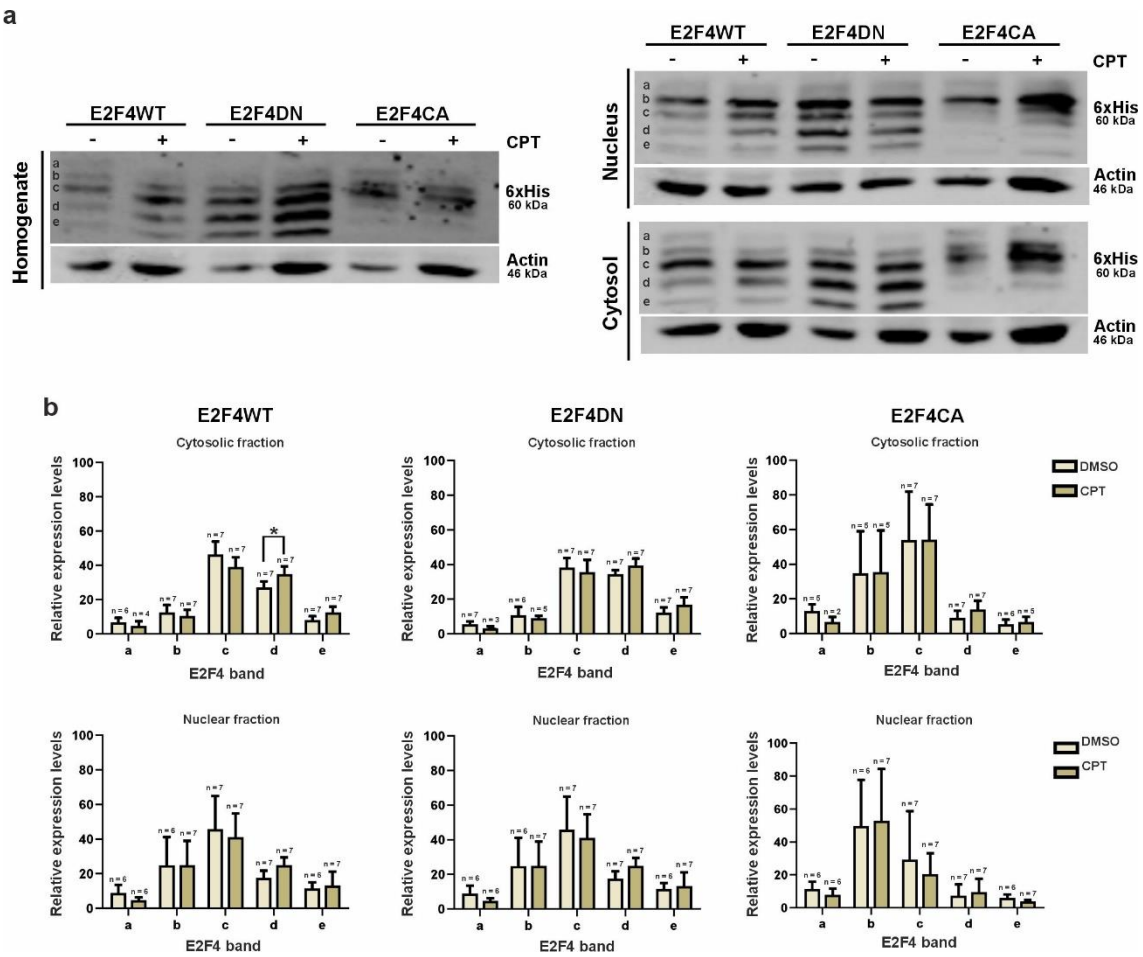

Figure 2. Subcellular localization of the different phosphorylation forms of E2F4 in N2a neurons. (a) Representative western blots of the multiband pattern detected in the indicated homogenates and subcellular fractions from E2F4WT-6xHis- (E2F4WT), E2F4DN-6xHis- (E2F4DN) or E2F4CA-6xHis-transduced N2a neurons (E2F4CA), either under control conditions or 8 h after CPT treatment, as revealed with an anti-6xHis antibody. Actin was used as a loading marker. Notice that the different forms of E2F4 are detected only in cytosol and nucleus. (b) Quantification of the relative frequency of the bands a-e that are present in the cytosolic and nuclear fractions for each experimental condition (see panel a). *$p<0.05$ [Two-way ANOVA, followed by Tukey's honestly significant difference (HSD) post-hoc test].

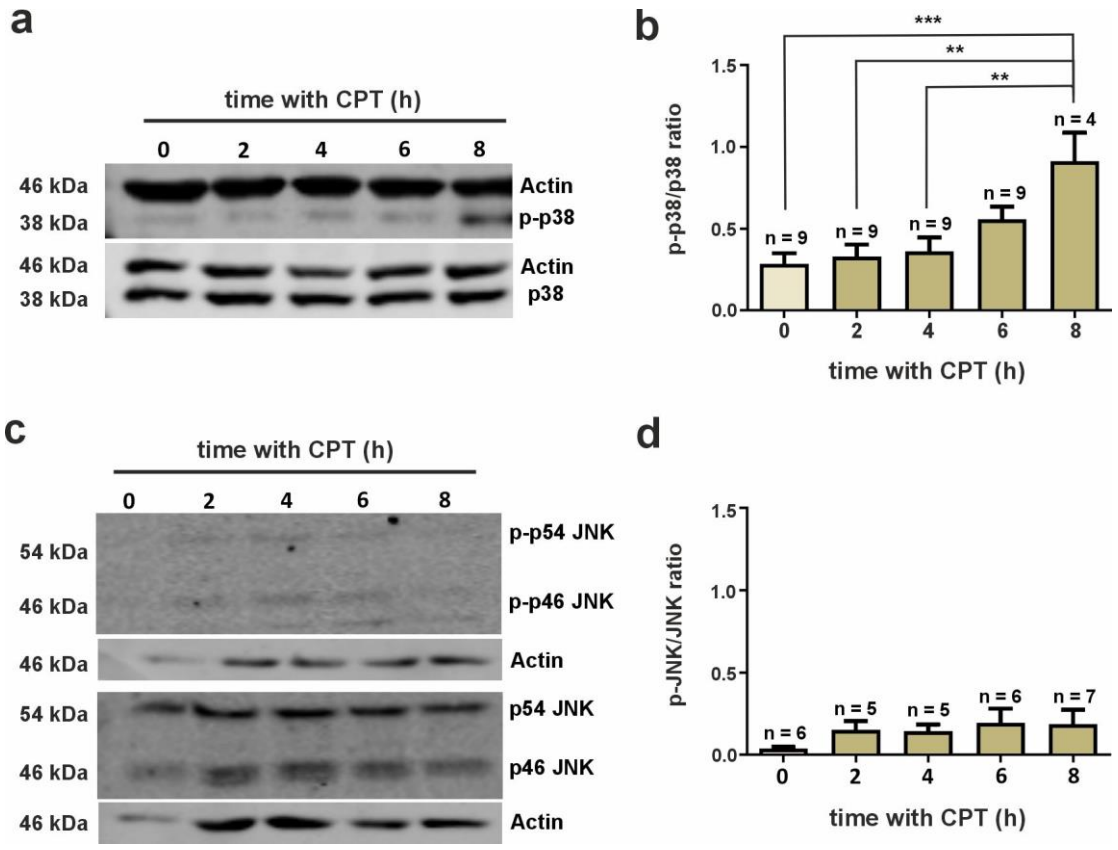

Figure 3. p38^{MAPK} activation in response to CPT in N2a neurons. (a) A Representative western blot from cell extracts of N2a neurons isolated at the indicated time points after 10 μM CPT treatment, using an antibody recognizing active p38^{MAPK} (p-p38) and total p38^{MAPK} (p38). Actin was used as a loading marker. (b) Quantification of p38^{MAPK} activation as the ratio between active p38^{MAPK} (relativized to Actin) and total p38^{MAPK} (relativized to Actin) at the indicated time points after CPT treatment. **$p<0.01$; ***$p<0.0001$ (One-way ANOVA, followed by Tukey's HSD post-hoc test). (c) Representative western blot from cell extracts of N2a neurons isolated at the indicated time points after 10 μM CPT treatment, using an antibody recognizing active JNK (p-p54 JNK and p-p46 JNK) and total JNK (p54 JNK and p46 JNK). Actin was used as a loading marker. (d) Quantification of JNK activation as the ratio between the sum of active JNK (p-p54 JNK plus p-p46 JNK relativized to Actin) and total p38^{MAPK} (p54 JNK plus p46 JNK relativized to Actin) at the indicated time points after CPT treatment.

a

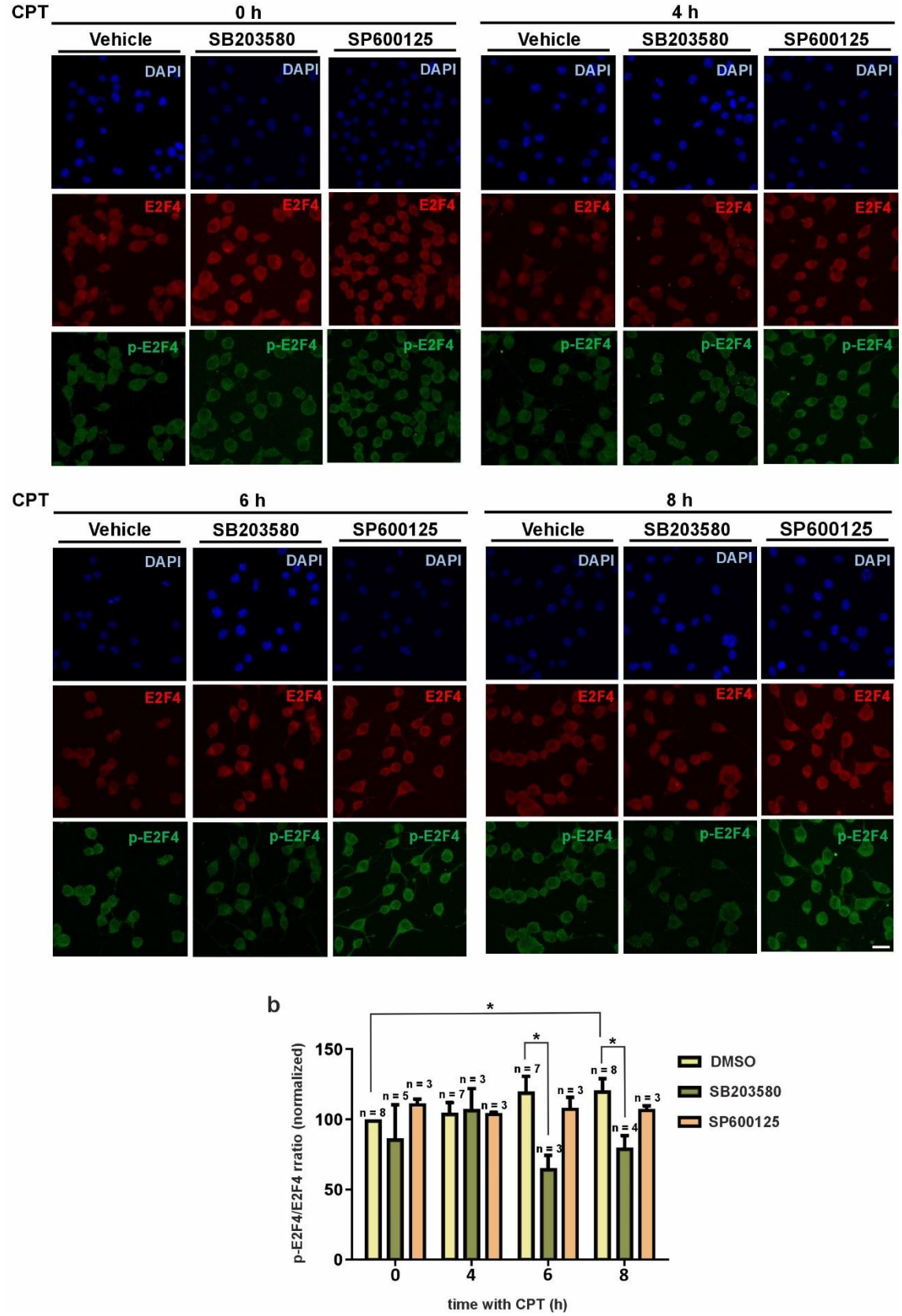
CPT
0 h
4 h
6 h
8 h
Vehicle
SB203580
SP600125
DAPI
E2F4
p-E2F4
b
p-E2F4/E2F4 rratio (normalized)
time with CPT (h)
DMSO
SB203580
SP600125
n = 8
n = 5
n = 3
n = 7
n = 4
*

Figure 4. E2F4 phosphorylation at Thr249 in N2a neurons treated with CPT. (a) Representative immunostaining of N2a neurons treated with 10 μM CPT for the indicated time points in the presence of vehicle, the $p38^{MAP}$ inhibitor SB203580 or the JNK inhibitor SP600125, using antibodies specific for total E2F4 (E2F4) or E2F4 phophorylated at Thr249 (P-E2F4). Cell nuclei were labeled with DAPI (blue) (b) Quantification of endogenous E2F4 phosphorylation at Thr249 of in response to 10 μM CPT treatment by measuring the ratio between p-E2F4 and E2F4 fluorescence intensities for each experimental condition. *$p<0.05$ (Two-way ANOVA, followed by Tukey's HSD post-hoc test).

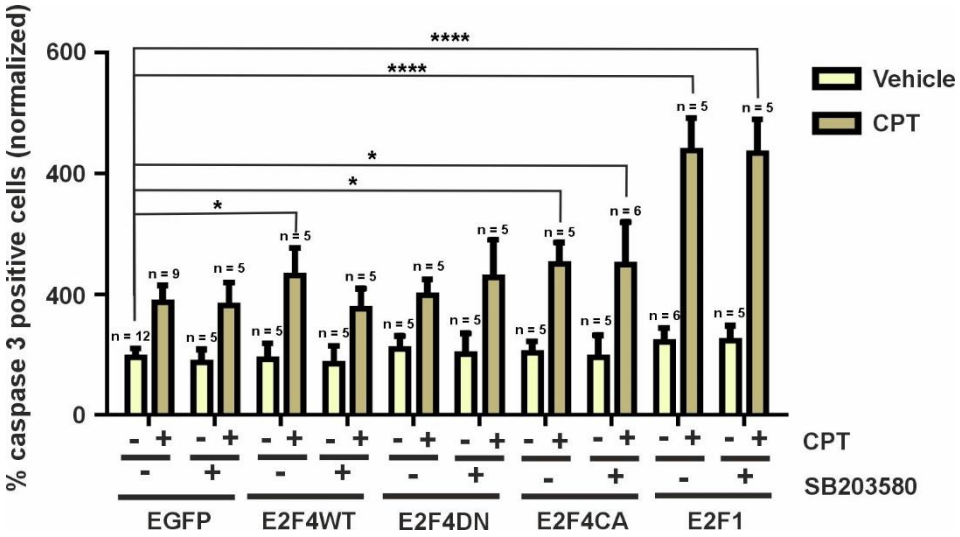

Figure 5. Regulation of apoptosis by E2F4 and E2F1 in CPT-treated N2a neurons. Quantification of active caspase-3-positive N2a neurons related to total DAPI-positive nuclei (see Fig. S5) for each indicated experimental condition, and normalized to the control condition (EGFP in the absence of both CPT and SB203580). *$p<0.05$; ****$p<0.00001$ (Two-way ANOVA, followed by Tukey's HSD post-hoc test).

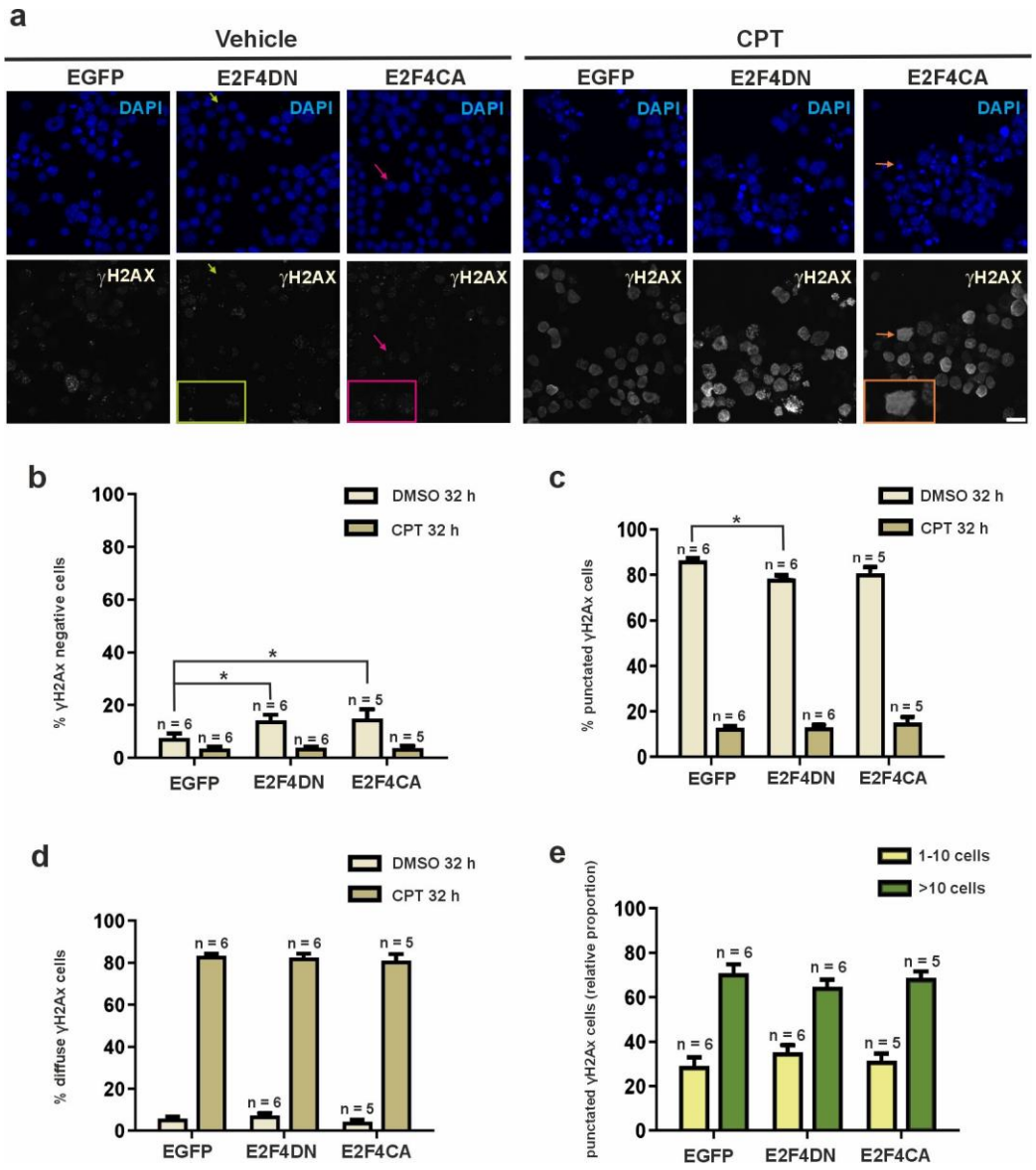

Figure 6. DNA damage regulation by E2F4 in N2a neurons. (a) Representative inmunostaining performed with an antibody specific for γH2AX to identify double strand breaks in the genomic DNA of N2a neurons transduced with either EGFP (EGFP), E2F4DN-6xHis (E2F4DN) or E2F4CA-6xHis (E2F4CA) and treated with 10 µM CPT for 32 h. Orange arrow: a γH2AX-positive cell with diffuse staining shown at high magnification in the orange box. Yellow arrow: a γH2AX-negative cell shown at high magnification in the green box. Pink arrow: a γH2AX-positive cell with punctate staining shown at high magnification in the pink box. Bar: 25 µM. (b) Quantification of the

γH2AX-negative N2a neurons, related to DAPI-positive nuclei, for each experimental group. (c) Quantification of the γH2AX-positive N2a neurons showing punctate staining, related to DAPI-positive nuclei, for each experimental group. (d) Quantification of the γH2AX-positive N2a neurons showing diffuse staining, related to DAPI-positive nuclei, for each experimental group. (e) Quantification of the proportion of γH2AX positive N2a neurons with punctate staining (1-10 vs. more than 10 foci) after being transduced with either EGFP, E2F4DN or E2F4CAXX and cultured for 32 h in the absence of CPT. *$p<0.05$ (Two-way ANOVA, followed by Tukey's HSD post-hoc test).

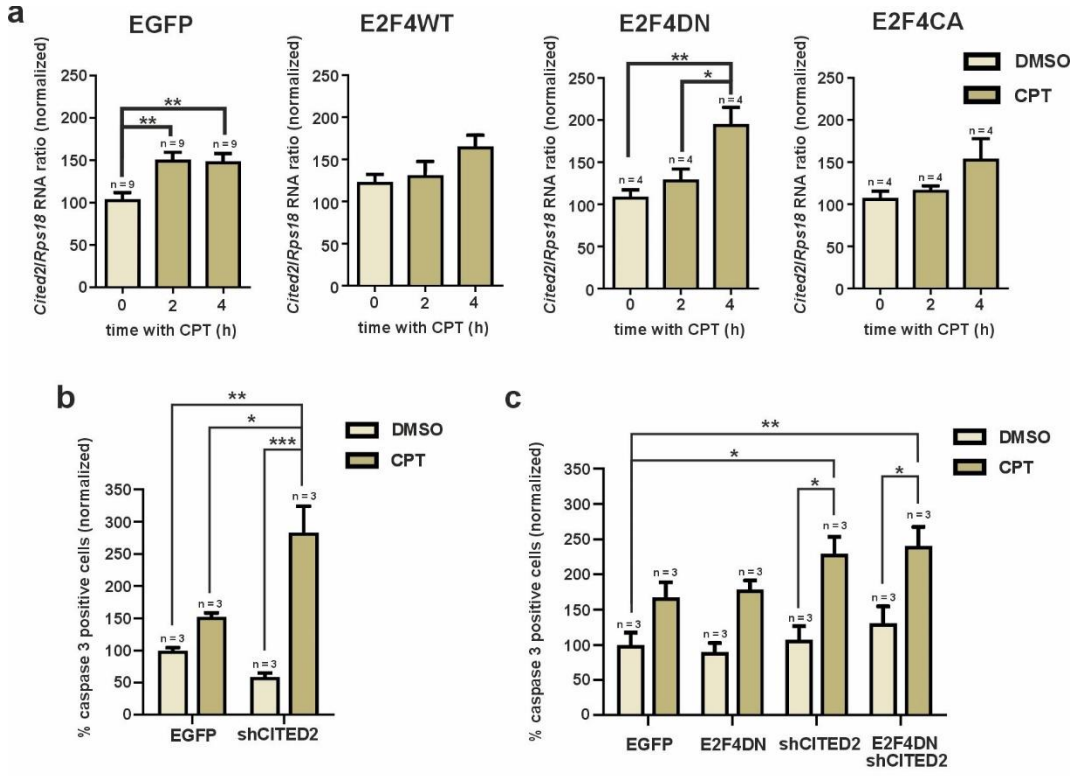

Figure 7. Participation of Cited2 in the apoptotic cell death regulated by E2F4 in N2a neurons. (a) Quantification of *Cited2* mRNA levels by real-time quantitative PCR (RT-qPCR), normalized to the *Rps18* housekeeping gene, in cDNA obtained from N2a neurons transduced with either EGFP (EGFP), E2F4WT-6xHis (E2F4WT), E2F4DN-6xHis (E2F4DN) or E2F4CA-6xHis (E2F4CA) treated for the indicated time periods with 10 µM CPT. *p<0.05; **p<0.01 (One-way ANOVA). (b) Quantification of active caspase-3-positive N2a neurons transduced with either EGFP or a *Cited2*-specific shRNA (shCITED2) and cultured for 32 h with 10 µM CPT, related to total DAPI-positive nuclei (see Fig. S5) and normalized to control conditions (EGFP/DMSO). (c) Quantification of active caspase-3-positive N2a neurons transduced with either 120 IU/cell of an Ad5.EGFP vector (EGFP), 60 IU/cell of an Ad5.E2F4DN-6xHis vector plus 60 IU/cell of an Ad5.EGFP vector (E2F4DN), 60 IU/cell of an Ad5 vector expressing a *Cited2*-specific shRNA plus 60 IU/cell of an Ad5.EGFP vector (shCITED2) or 60 IU/cell of an Ad5.E2F4DN-6xHis vector plus 60 IU/cell of an Ad5 vector expressing a *Cited2*-specific

shRNA (E2F4DN/shCITED2) and cultured for 32 h with 10 μM CPT, related to total DAPI-positive nuclei. *$p<0.05$; **$p<0.01$; ***$p<0.001$ (Two-way ANOVA, followed by Tukey's HSD post-hoc test).

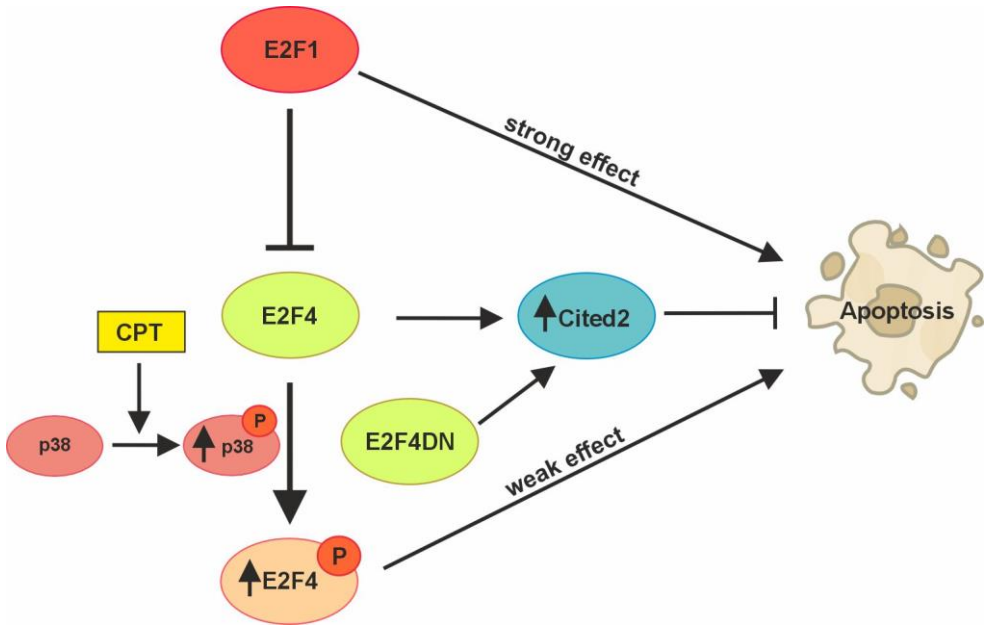

Figure 8. Scheme illustrating the proposed mechanism of E2F4DN to favor the survival of CPT-treated N2a neurons. Under normal conditions, E2F4 facilitates the expression of Cited2, which trigger antiapoptotic signaling in N2a neurons. Genotoxic stress induced by CPT leads to $p38^{MAPK}$ activation, which phosphorylates E2F4 at the Thr249/Thr251 motif. This facilitates a weak proapoptotic effect of E2F4 that mimics the effect of E2F1 as a strong proapoptotic trigger in CPT-treated cells. E2F4DN, which cannot be phosphorylated at the Thr249/Thr251 motif, maintains the capacity of E2F4 to induce Cited2 expression and the antiapoptotic effect of the latter.

Supplemental figures

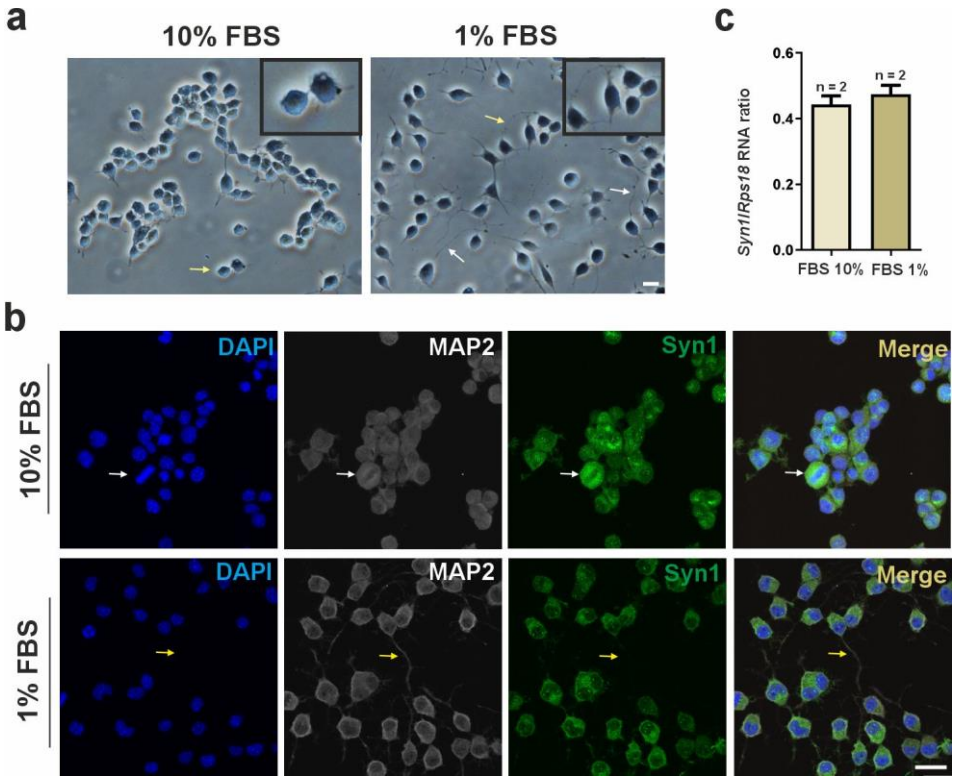

Figure S1. Differentiation of N2a neuroblastoma cells into N2a neurons. (a) Representative bright field images of N2a neuroblastoma cells cultured with DMEM supplemented with FBS 10% (10 % FBS) or FBS 1% (1% FBS). Box: high magnification to visualize the neurites that can be observed in N2a neuroblastoma cells cultured with 1% FBS (i.e. N2a neurons). (b) Representative immunostaining of N2a neuroblastoma cells cultured with 10% FBS or 1% FBS, using antibodies for the neuronal markers MAP2 (MAP2) and Synapsin 1 (Syn1). Cell nuclei were labeled with DAPI (blue). White arrow: mitotic cell in the presence of 10% FBS. Yellow arrow: MAP2-positive process. (c) Quantification of *Syn1* mRNA by real-time quantitative PCR (RT-qPCR) normalized to the *Rps18* housekeeping gene in cDNA obtained from N2a neurons cultured with either FBS 10% or FBS 1%.

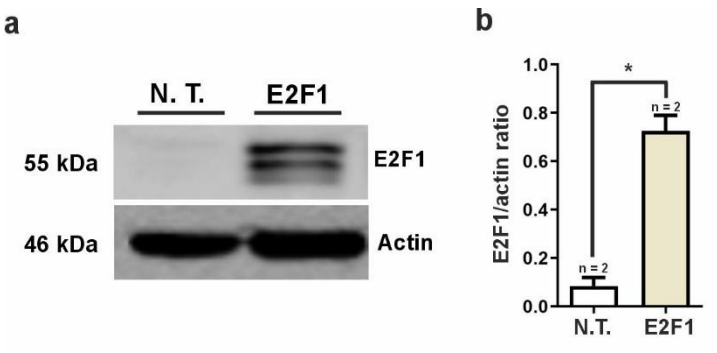

Figure S2. Overexpression and phosphorylation of E2F1 in N2a neurons. (a) Representative western blot of cell extracts from N2a neurons either non-transduced (N.T.) or transduced with an Ad5.HA-E2F1 vector (E2F1) using antibodies against E2F1 and actin. Notice that exogenous E2F1show a multiple band pattern, likely due to phosphorylation. (b) Quantification of the E2F1 protein level relativized to actin in cell extracts from N2a neurons either non-transduced (N.T.) or transduced with an Ad5.HA-E2F1 vector (E2F1). *$p<0.05$ (unpaired Student's *t* test).

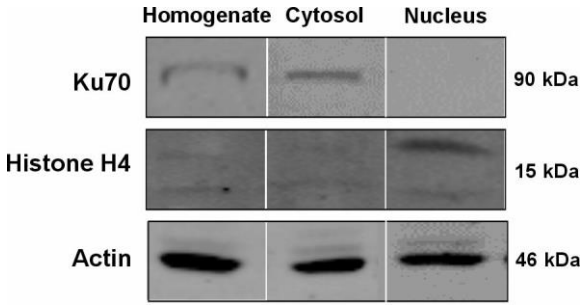

Figure S3. Cellular fractionation markers in N2a neurons. Representative western blots of whole cell extracts (homogenates) and the indicated subcellular fractions from N2a neurons, using antibodies against Ku70, Histone H4 and Actin. Notice that the cytosolic fraction contains Ku70, whereas the nuclear fraction contains Histone H4. Actin was used as a loading marker.

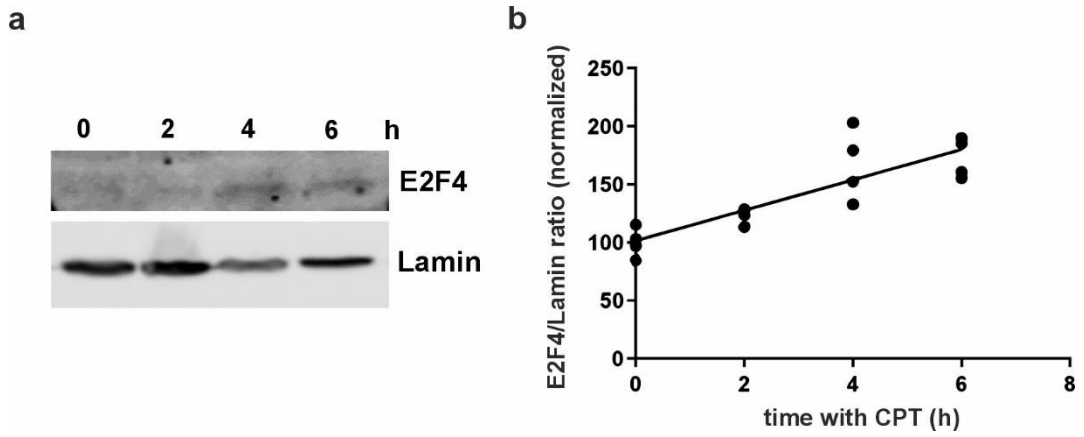

Figure S4. Increase of E2F4 protein in CPT-treated N2a neurons. (a) Representative western blot of cell extracts from N2a neurons at the indicated time points after 10 μM CPT treatment, using an anti-E2F4-specific antibody. Actin was used as a loading marker. (b) Regression analysis of the E2F4 protein levels at the indicated time points after 10 μM CPT treatment. R^2=0.9646; p=0.0354.

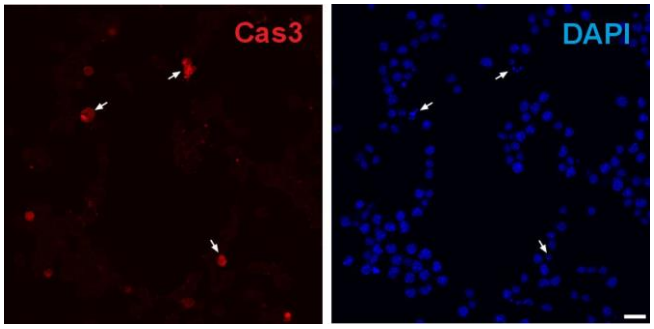

Figure S5. Active caspase-3 lebeling in N2a neurons. Example of N2a neurons immunostained with an antibody specific for active caspase-3 (red). Cell nuclei were labeled with DAPI (blue) to identify pyknotic nuclei. Arrows: pyknotic nuclei positive for active caspase-3 (Cas3) labeling. Bar: 25 μM.

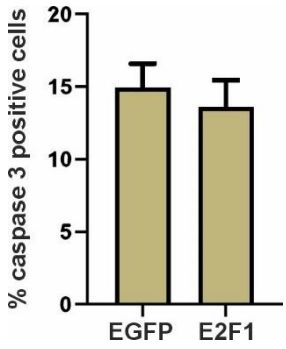

Figure S6. Caspase 3 cleavage regulation by E2F1 in N2a derived neurons. Quantification of active caspase-3-positive N2a neurons transduced with either EGFP or E2F1 and treated for 24 h with 10 µM CPT, related to total DAPI-positive nuclei.

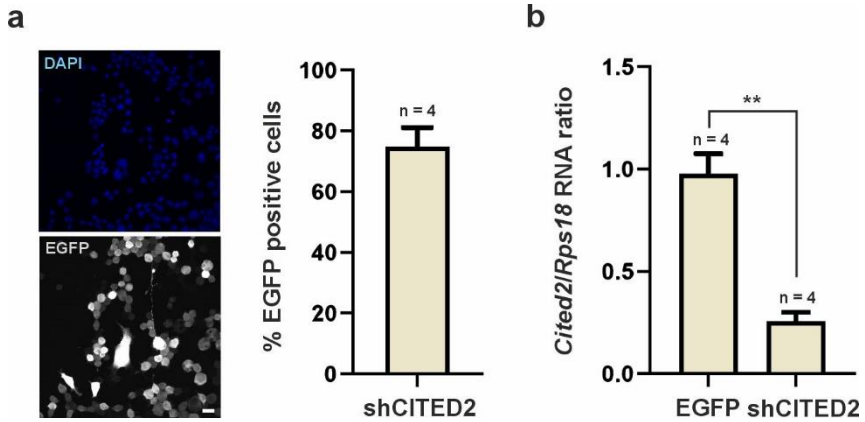

Figure S7. Regulation of *Cited2* expression by a *Cited2*-specific shRNA in N2a neurons. (a) Left panel: representative immunostaining of N2a neurons transduced with an Ad5 vector co-expressing a *Cited2*-specific shRNA together with EGFP, using antibodies against EGFP. Cell nuclei were labeled with DAPI (blue). Right panel: quantification of EGFP-positive N2a neurons related to DAPI-positive nuclei. (b) Quantification of *Cited2* mRNA by RT-qPCR normalized to the *Rps18* housekeeping gene in cDNA obtained from N2a neurons transduced with either EGFP or an Ad5 vector co-expressing a *Cited2*-specific shRNA together with EGFP.